Steamed broccoli sprouts alleviate DSS-induced inflammation and retain gut microbial biogeography in mice.

Johanna M. Holman[1], Louisa Colucci[2], Dorien Baudewyns[3], Joe Balkan[4], Timothy Hunt[5], Benjamin Hunt[5], Marissa Kinney[1], Lola Holcomb[6], Grace Chen[7], Peter L. Moses[8,9], Gary M. Mawe[8], Tao Zhang[10], Yanyan Li[1*], Suzanne L. Ishaq[1*]

[1] School of Food and Agriculture, University of Maine, Orono, Maine, USA 04469
[2] Department of Biology, Husson University, Bangor, Maine, USA 04401
[3] Department of Psychology, University of Maine, Orono, USA 04469
[4] Department of Chemical and Biological Engineering, Tufts University, Medford, Massachusetts, USA 02155
[5] Department of Biology, University of Maine, Orono, Maine, USA 04469
[6] Graduate School of Biomedical Sciences and Engineering, University of Maine, Orono, Maine, USA 04469
[7] Department of Internal Medicine, University of Michigan Medical School, Ann Arbor, Michigan, USA 48109
[8] Departments of Neurological Sciences and of Medicine, Larner College of Medicine, University of Vermont, Burlington, Vermont, USA 05401
[9] Finch Therapeutics, Somerville, Massachusetts, USA 02143
[10] School of Pharmacy and Pharmaceutical Sciences, SUNY Binghamton University, Johnson City, New York, USA 13790

***Corresponding authors:**
Suzanne L. Ishaq, University of Maine, School of Food and Agriculture, Orono, ME 04469, sue.ishaq@maine.edu, 1-207-581-2770
Yanyan Li, University of Maine, School of Food and Agriculture, Orono, ME 04469, yanyan.li@maine.edu, 1-207-581-3134

Keywords: inflammatory bowel disease, ulcerative colitis, broccoli sprouts, sulforaphane, glucoraphanin, gut microbiota, dietary bioactives, biogeography, *Bacteroides thetaiotaomicron*.

Abstract: Inflammatory Bowel Diseases (IBD) are devastating conditions of the gastrointestinal tract with limited treatments, and dietary intervention may be effective, and affordable, for managing symptoms. Glucosinolate compounds are highly concentrated in broccoli sprouts, especially glucoraphanin, and can be metabolized by certain mammalian gut bacteria into anti-inflammatory isothiocyanates, such as sulforaphane. Gut microbiota exhibit biogeographic patterns, but it is unknown if colitis alters these or whether the location of glucoraphanin-metabolizing bacteria affects anti-inflammatory benefits. We fed specific pathogen free C57BL/6 mice either a control diet or a 10% steamed broccoli sprout diet, and gave a three-cycle regimen of 2.5% dextran sodium sulfate (DSS) in drinking water over a 34-day experiment to simulate chronic, relapsing ulcerative colitis. We monitored body weight, fecal characteristics, lipocalin, serum cytokines, and bacterial communities from the luminal- and mucosa-associated populations in the jejunum, cecum, and colon. Mice fed the broccoli sprout diet with DSS treatment performed better than mice fed the control diet with DSS, including significantly more weight gain, lower Disease Activity Indexes, lower plasma lipocalin and proinflammatory cytokines, and higher bacterial richness in all gut locations. Bacterial communities were assorted by gut location, but were more homogenous across locations in the control diet + DSS mice. Importantly, our results showed that broccoli sprout feeding abrogated the effects of DSS on gut microbiota, as bacterial richness and biogeography were similar between mice receiving broccoli sprouts with and without DSS. Collectively, these results support the protective effect of steamed broccoli sprouts against dysbiosis and colitis induced by DSS.

Importance: Evaluating bacterial communities across different locations in the gut provides a greater insight than fecal samples alone, and provides an additional metric by which to evaluate

59 beneficial host-microbe interactions. Here, we show that 10% steamed broccoli sprouts in the diet
60 protects mice from the negative effects of dextran sodium sulfate induced colitis, that colitis erases
61 biogeographical patterns of bacterial communities in the gut, and that the cecum is not likely to be
62 a significant contributor to colonic bacteria of interest in the DSS mouse model of ulcerative colitis.
63 Mice fed the broccoli sprout diet during colitis performed better than mice fed the control diet
64 while receiving DSS. The identification of accessible dietary components and concentrations that
65 help maintain and correct the gut microbiome may provide universal and equitable approaches to
66 IBD prevention and recovery, and broccoli sprouts represent a promising strategy.

67

68 **Introduction**

69 Inflammatory Bowel Diseases (IBD) are globally prevalent, chronic inflammatory diseases
70 of multifactorial origin which disrupts daily life and creates financial burdens to individuals and
71 healthcare systems (1, 2). IBD symptoms occur in the gastrointestinal (GI) tract, and can be
72 accompanied by immune dysfunction (3) and microbial community changes in the gut. In addition
73 to being debilitating, a longer duration of IBD is associated with an increased risk of developing
74 GI cancers (4). Treatments are currently limited to alleviating inflammation and returning patients
75 to as close to homeostasis as possible. Diet can play an important role in the management of IBD
76 as a source of anti-inflammatory metabolites, and as a tool for influencing the robustness of gut
77 microbiomes. However, many guidelines for IBD patients recommend avoiding high-fiber or
78 sulfur-rich foods which produce metabolites that could exacerbate symptoms (5). Diet can be
79 beneficial (6) or detrimental to gut inflammation (7), but IBD patients may choose to avoid most
80 fiber- or sulfur-rich foods rather than test their reaction to specific foods (8). Thus, a better

81 understanding of the interaction of diet, gut microbiota, and disease is needed before dietary
82 recommendations can be made.

83 Diets which are high in cruciferous vegetables, such as broccoli, are associated with
84 reduced inflammation and cancer risk, e.g. (9–11), due to a group of specific plant secondary
85 compounds, glucosinolates. Glucosinolates are very high in broccoli, especially seeds or immature
86 sprouts, and can be converted into bioactive metabolites (12, 13), such as sulfur-containing
87 isothiocyanates, by the action of myrosinase, an enzyme present in these vegetables.
88 Isothiocyanates are used by the plant for defense against insect herbivory, but in humans, have
89 been identified as bioactive candidates for reducing gut inflammation (14–16). Specifically,
90 sulforaphane (SFN), a well-studied isothiocyanate (17), has been shown to inhibit the action of
91 immune factors which are responsible for upregulation of several proinflammatory cytokines;
92 interleukins-6, -8, -12, -21, and -23 (11, 18, 19), which has recently been evaluated as a possible
93 strategy for reducing gut inflammation in humans and mouse models (13, 14, 16).

94 However, consuming raw broccoli and broccoli sprouts results in small amounts of
95 available SFN, as broccoli-sourced enzymes preferentially metabolize the precursor,
96 glucoraphanin (GLR), to an inactive byproduct instead (17). Cooking the sprouts alters the activity
97 of plant enzymes to prevent the creation of the inactive byproduct, leaving glucosinolates intact
98 (13, 20). Mammals do not produce the enzymes for converting glucosinolates to isothiocyanates;
99 however, gut bacteria with β-thioglucosidase activity can cleave the glycoside moiety from
100 glucosinolates, and there is evidence for GLR hydrolysis to SFN by colonic and cecal bacteria, *ex*
101 *vivo* and *in vivo* in humans and animal models, e.g. (13, 15, 17). The bacteria and genes that are
102 capable of metabolizing glucosinolates are not fully known, but strains of *Lactobacillus*,
103 *Bifidobacteria, Bacteroides,* and other genera have been implicated (15, 21, 22), with the most

104 known about the genes in *Bacteroides thetaiotaomicron (21)*. Moreover, the conditions in the gut
105 (e.g., diet, inflammation) under which this glucosinolate metabolism by bacteria occurs or not are
106 not well understood. For example, people consuming cooked broccoli stopped excreting
107 isothiocyanates in their urine after being treated with oral antibiotics and bowel cleansing which
108 reduced gut bacterial diversity and biomass (23). Further, not everyone's gut bacteria can be
109 reliably induced to meaningful levels of GLR conversion (24, 25). Thus, bacterial metabolism of
110 GLR to SFN *in situ* must be better understood prior to making dietary recommendations.

111 Mouse studies suggest that biotransformation of GLR to SFN occurs in the colon (13, 21,
112 26), and we confirmed that the majority of SFN accumulation occurs in the colon by using multiple
113 locations of measurement along the GI tract (13). The microbial communities along the GI tract
114 are highly dependent on the diet, health status, age, and microbial encounters of the host (27, 28).
115 Additionally, each organ in the GI tract and sites within organs foster different environmental
116 conditions that create spatial niches for different microbial taxa, an ecological pattern known as
117 biogeography (29, 30). However, changes to conditions in one location may have repercussions
118 downstream. For example, a low pH in the stomach results in low bacterial diversity and biomass
119 in the duodenum (31). IBD patients often have a less acidic GI tract (32) due to altered diet or
120 treatments, and this allows more bacteria to survive transit through the stomach which may result
121 in small intestinal bacterial overgrowth (33), especially in mucosal-associated fractions (34–36).
122 Moreover, the bacterial communities in the colon of IBD patients are disrupted (37), but this may
123 result from inflammation and disruption to host-microbial relations in the colon itself or from
124 further upstream (34, 38). Thus, changing the biogeography of gut bacterial communities in IBD
125 patients could alter the dynamics of SFN production, which could improve or lessen the benefits
126 to the host of having this anti-inflammatory produced in the gut.

127 Steamed broccoli sprouts provided in the diet of mice has been demonstrated to reduce
128 inflammation in mice with chemically induced colitis (13); however, there are significant
129 knowledge gaps regarding the effect of broccoli sprouts on the gut microbiota. In particular, there
130 are gaps regarding bacterial biogeography in general and that of the glucosinolate-metabolizing
131 taxa specifically, and how this may impact health benefits to the host. To address these, we
132 assessed the impact of steamed broccoli sprouts on the biogeographic pattern of gut microbiota
133 and disease outcome in a mouse model of chronic, relapsing colitis. We fed specific pathogen free
134 (SPF) C57BL/6 mice either a control diet or a 10% steamed broccoli sprout diet balanced by
135 macronutrient and by fiber, starting at 7 weeks of age and continuing for another 34 days. The
136 fresh broccoli sprouts were steamed to inactivate plant enzymes, and thus the metabolism of
137 glucosinolates to isothiocyanates would rely on the gut microbiota. A three-cycle regimen of
138 dextran sodium sulfate (DSS) in drinking water was given to stimulate chronic colitis in the mice,
139 which is a well-established method for modeling ulcerative colitis (39–41). We analyzed the
140 bacterial communities from the luminal-associated (i.e., digesta contents) and mucosal-associated
141 (i.e., epithelial scrapings) fractions in the jejunum, cecum, and colon using 16S rRNA gene
142 sequencing, and correlated these communities with metrics of disease activity including weight
143 gain/stagnation, fecal characteristics, lipocalin (as a surrogate marker for inflammation in IBD),
144 and proinflammatory cytokines (Figure 1).
145

146 **Results**

147 **Broccoli sprouts alleviated disease characteristics of DSS-induced colitis**

148 After 1 week of acclimatization to the facility, forty (40) 7-week-old SPF C57BL/6 mice
149 were divided into four groups: control diet (Control), control diet with 2.5% DSS in drinking water

150 (Control+DSS), 10% (w/w) steamed broccoli sprout diet (Broccoli, with the control diet as the
151 base), and 10% broccoli sprout diet with 2.5% DSS in drinking water (Broccoli+DSS). Over 34
152 days of the diet treatments, the two groups of mice receiving DSS were exposed to three cycles
153 (days 8-12, 18-22, 30-34) designed to induce chronic, relapsing colitis (48, Figure 1). Periodically
154 throughout the experiment, mice were monitored for weight loss, fecal blood, and fecal
155 consistency. After euthanasia (day 34), samples were collected for analyses including: plasma
156 lipocalin, plasma cytokines, and DNA extraction and community sequencing of lumen-associated
157 (digesta contents) and mucosal-associated (epithelial scrapings) from the jejunum, cecum
158 (contents only), and colon.

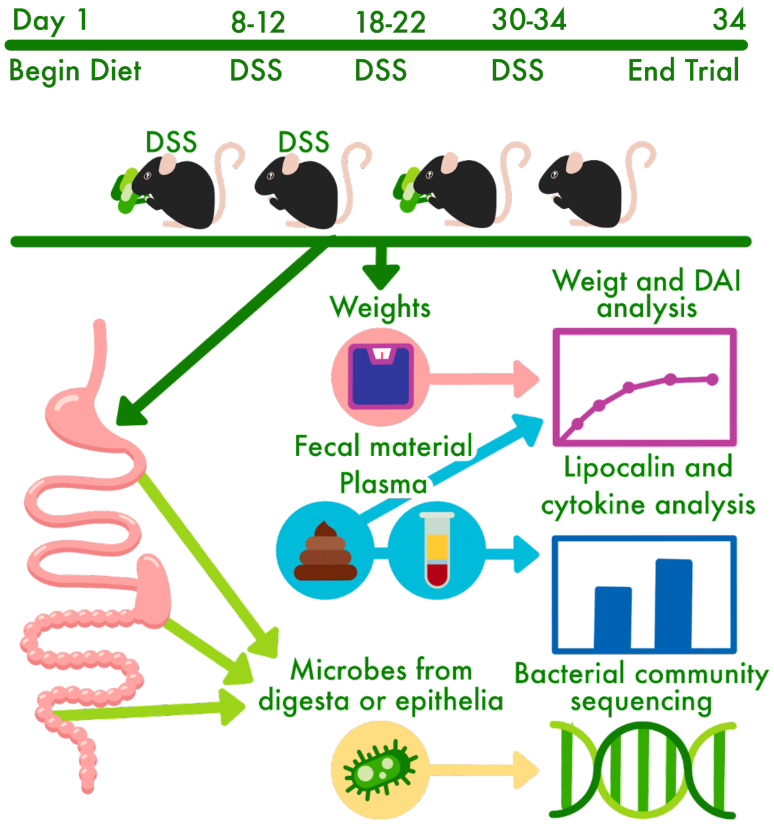

159

160 **Figure 1. Experimental design schematic for a chronic model of ulcerative colitis induced by**
161 **dextran sodium sulfate (DSS) in 40 male mice (C57BL/6) beginning at 7-weeks of age.**
162

163 ***Weight.*** Mice with induced colitis and fed the broccoli sprout diet (Broccoli+DSS) gained
164 significantly more weight than the mice with induced colitis on the control diet (Control+DSS)
165 (Figure 2A; ANOVA, $p < 0.03$). Further, the weight gain of Broccoli+DSS mice was statistically
166 similar to that for the two diet groups without DSS treatment (Figure 2A; ANOVA, $p > 0.05$). All
167 the juvenile mice gained some weight as they were in a growth phase; despite this, the first two
168 DSS cycles resulted in weight loss, especially in the Control+DSS group. The Broccoli+DSS mice
169 recovered this weight loss prior to the beginning of the next cycle, but the Control+DSS mice did
170 not (Figure 2A). At the beginning of the third and last DSS cycle, the mice were reaching maturity
171 at eleven (11) weeks old and the weights of all groups were somewhat constant. However, the
172 Control+DSS group demonstrated a significantly lower weight at the end of the study than the
173 other groups which were statistically similar (Figure 2A).

174 ***Disease Activity Index.*** Mice in the Broccoli+DSS group demonstrated significantly lower
175 Disease Activity Index scores (DAI; including scoring weight loss, fecal blood, and fecal
176 consistency) than the mice in the Control+DSS group during DSS cycle 2 and 3, but were similar
177 in cycle 1 (Figure 2B). The Broccoli+DSS DAI scores were significantly elevated on four days
178 during the trial (see Figure 2B; ANOVA, $p < 0.05$, comparisons by treatment, adjusted with
179 TukeyHSD for multiple comparisons), as well as in an additive model considering the data over
180 the entire study (GAM, $F = 17.47$, $p < 0.001$), however returned to near 0 during rest periods
181 between DSS cycles. Mice in the Control+DSS group demonstrated elevated DAI scores from
182 DSS cycle 1 and remained high throughout the study (Figure 2B), including during rest periods.
183 The elevated scores were significant on many dates (see ***, Figure 2B) as compared to the mice
184 in the Control group (Figure 2B, ANOVA, $p < 0.05$, comparisons by day, adjusted with TukeyHSD
185 for multiple comparisons), as well as in an additive model considering the data over the entire

study (GAM, $F = 308.32$, $p < 0.001$). The Control and Broccoli diet groups had statistically similar scores which were at or nearly 0, at the end of the trial (ANOVA, $p > 0.05$) or over time (GAM, $p > 0.05$).

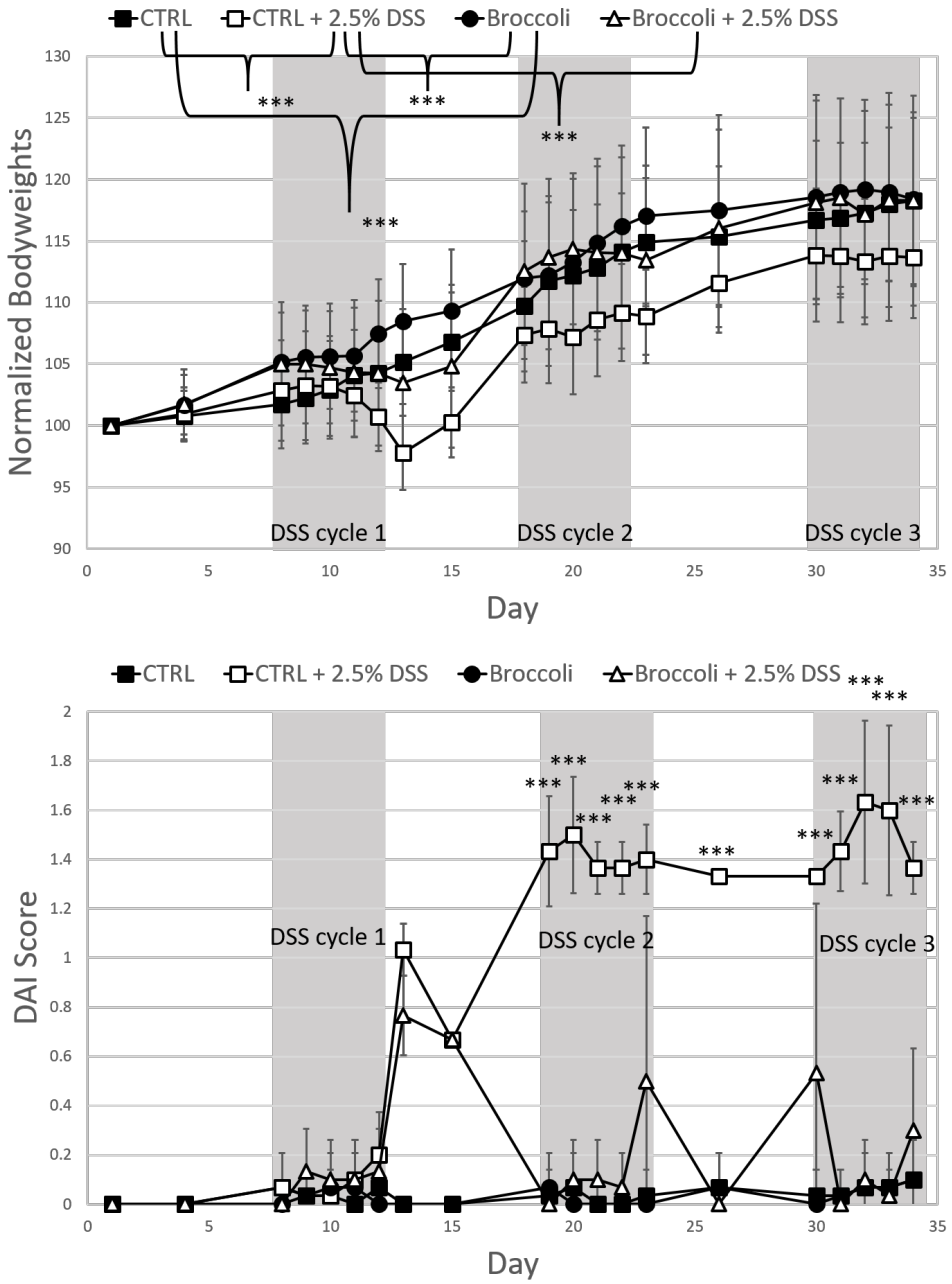

Figure 2. Body weights (A) and Disease Activity Index scores (B) in mice across a 34-day trial under a DSS-induced model of chronic, relapsing colitis with or without 10% steamed broccoli sprouts in diet. Body weights and time scale were normalized to the day mice began the broccoli sprout diet, set at 100% starting weight and Day 1, respectively. DAI scores are calculated

194 by weight loss intensity score, fecal blood, and fecal consistency. Treatment comparisons at each
195 day compared by ANOVA, and significance is designated as 0.001 '***'.
196
197

198

199 ***Proinflammatory cytokines.*** Mice in the Broccoli+DSS group indicated significantly
200 lower levels of proinflammatory cytokines IL-1β, IL-6 and TNF-α in plasma than mice in the
201 Control+DSS group (Figure 3A). The plasma levels of IL-1β and TNF-α were similar across the
202 Broccoli+DSS, Broccoli, and Control groups, and the IL-6 measure was slightly elevated (Figure
203 3A). The cytokine CCL4, also known as macrophage inflammatory protein 1β (MIP1β) and which
204 is a chemokine that plays a critical role in regulating the migration and activation of immune cells
205 during inflammatory processes (42), did not differ significantly among the four treatment groups
206 (Figure 3A).

207 ***Plasma lipocalin.*** At the end of DSS cycle 3, plasma lipocalin (LCN2) levels in the
208 Broccoli+DSS mice were not significantly different from the groups without DSS, and were
209 significantly lower in comparison with the Control+DSS group (ANOVA, $p < 0.05$, Figure 3B).

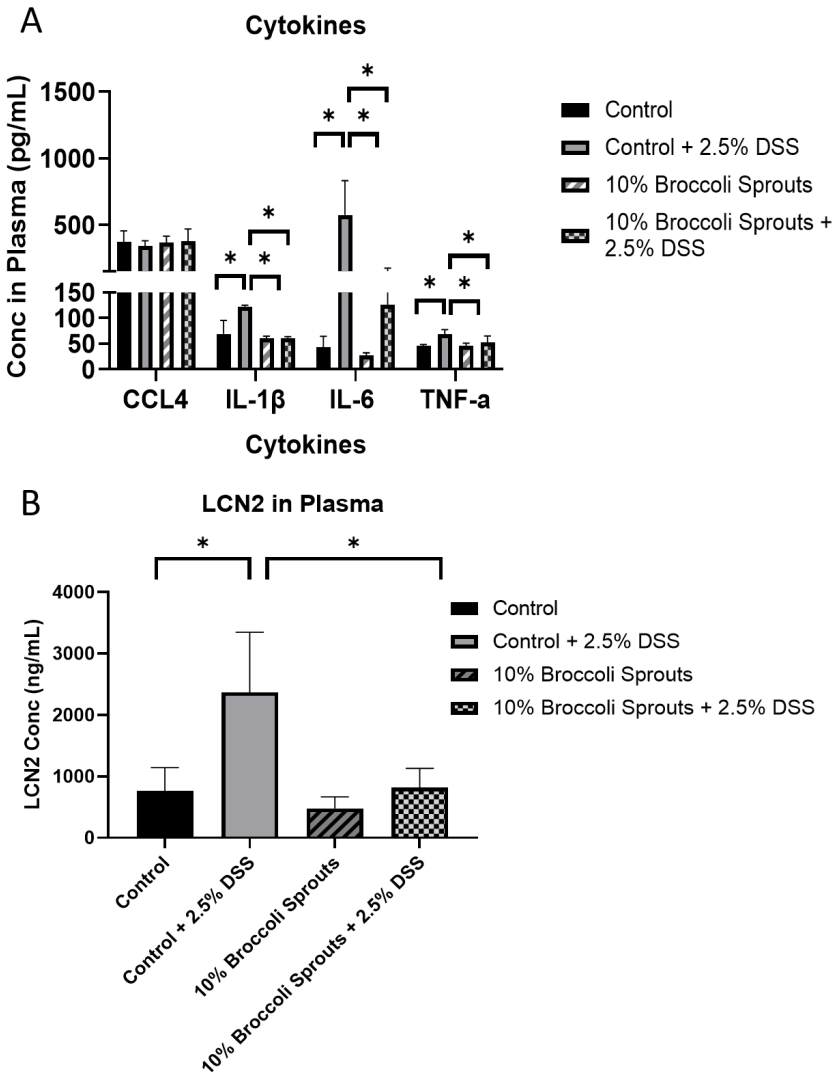

Figure 3 Cytokines (A) and lipocalin (B) in plasma on the last day of the trial from mice under a DSS-induced model of chronic, relapsing colitis with or without 10% steamed broccoli sprouts in diet. Cytokines include CCL4; interleukins IL-1β and IL-6; and tumor necrosis factor alpha (TNF-α). Data are represented as mean ± SD. *, $p < 0.05$, ANOVA.

Fecal blood correlated with bacterial taxa. Mice in the Broccoli+DSS group with positive fecal occult blood scores demonstrated some differential bacteria compared to mice in the Control+DSS group with positive blood scores (Figure 4). The most abundant of these differential bacterial sequence variants (SV) in the Broccoli+DSS group were in the Muribaculaceae family

and the *Clostridium* sensu stricto [Latin: strictly speaking] clade (Figure 4). The Control+DSS mice indicated different SVs with the most abundant in the *Clostridium* sensu stricto clade and *Cutibacterium* (Figure 4).

Figure 4. Gut bacterial taxa identified from mice having a positive fecal occult blood score at sacrifice under a DSS-induced model of chronic, relapsing colitis with or without 10% steamed broccoli sprouts in diet. Data were subset to mice with a positive score on the last day of the experiment, when the gut samples were collected. Important features (SVs) were identified

through permutational random forest analysis, and only the features important to this group (>50 reads) are listed out of 143 significant ($p < 0.05$) features across all treatments. Model accuracy was 89.7%. Bacterial sequence variants (SV) are identified as the lowest level of taxonomic identity possible, with "NA" indicating which could not be identified to species, and the number indicating which specific SV it was.

Broccoli sprouts protected against DSS-induced changes to bacterial communities

Bacterial richness. Mice with induced colitis on the broccoli sprouts diet (Broccoli+DSS) demonstrated significantly more bacterial richness in the cecal contents, colon contents, and colon scrapings than mice without broccoli sprouts (Control+DSS, Figure 5, Table 1). Across all treatments and all anatomical sites (jejunum contents & scrapings, cecal contents, colon contents & scrapings), bacteria were primarily identified as belonging to the phyla Firmicutes/Bacillota, Bacteroidetes/Bacteroidota, Proteobacteria/Pseudomonadota, Actinobacteria/Actinomycetota (which was highest in Control+DSS mice), and Verrucomicrobia/Verrucomicrobiota (which was highest in mice consuming broccoli sprouts; (Figure S1). The two groups receiving broccoli sprouts had the highest bacterial richness in all gut locations, particularly in the colon contents and scrapings (Figure 5). In comparison to the Control group, the Control+DSS mice demonstrated higher bacterial richness in the jejunum, lower richness in the cecal contents, and comparable bacterial richness in the colon (Figure 5). In addition, the Control+DSS mice had similar median richness in the jejunum, cecum, and colon contents, with the widest distribution of richness in the jejunum and colon (Figure 5). Moreover, the Control+DSS richness was similar between the digesta contents and epithelial scraping sites, in both the jejunum and in the colon, implying homogenization of bacterial communities in those sites (Figure 5).

Figure 5. Observed bacterial richness along the intestine of mice under a DSS-induced model of chronic, relapsing colitis with or without 10% steamed broccoli sprouts in diet. Richness is calculated as the number of different bacterial sequence variants (SVs). Statistically significant comparisons are provided in Table 1.

Table 1. Statistical comparison of observed richness along the intestine of mice under a DSS-induced model of chronic, relapsing colitis with or without 10% steamed broccoli sprouts in diet. Comparisons were made using linear regression models comparing treatment, in subsets of the data by anatomical location. Only significant comparisons ($p < 0.05$) are listed. Bacterial richness is visualized in Figure 5.

Treatment compared to control diet only group	**Change in bacterial richness (SVs) ± Standard Error (rounded)**	**T-value**	**P-value**
	Jejunum contents		
Control + 2.5% DSS	40 ± 11	3.790	0.000608 ***

10% Broccoli sprouts	23 ± 10	2.766	0.009207 **
10% Broccoli sprouts + 2.5% DSS	64 ± 10	6.141	5.05e-07 ***
Jejunum scraping			
Control + 2.5% DSS	52 ± 17	3.`04	0.00434 **
10% Broccoli sprouts	98 ± 16	6.230	1.16e-06 ***
10% Broccoli sprouts + 2.5% DSS	100 ± 15	6.708	3.35e-07 ***
Cecum contents			
Control + 2.5% DSS	-13 ± 15	-0.821	0.418
10% Broccoli sprouts	68 ± 13	5.120	1.54e-05 ***
10% Broccoli sprouts + 2.5% DSS	70 ± 13	5.225	1.54e-05 ***
Colon contents			
Control + 2.5% DSS	-12 ± 9	-1.316	0.197
10% Broccoli sprouts	43 ± 9	4.525	6.67e-05 ***
10% Broccoli sprouts + 2.5% DSS	90 ± 10	9.172	7.74e-11 ***
Colon scraping			
Control + 2.5% DSS	14 ± 12	1.225	0.129
10% Broccoli sprouts	60 ± 12	5.220	1.78e-05 ***
10% Broccoli sprouts + 2.5% DSS	89 ± 12	7.749	2.81e-08 ***

262

263 ***Beta diversity.*** Mice in the Broccoli+DSS group displayed a bacterial community that was
264 distinct from that of mice in the Control+DSS group (Figure 6A,B). Bacterial taxa were
265 characterized based on presence/absence (unweighted Jaccard Similarity, permANOVA: $F =$
266 16.90, $p < 0.001$) and presence/abundance (weighted Bray-Curtis Similarity, permANOVA: $F =$
267 29.97 $p < 0.001$). Interestingly, the bacterial community of the Broccoli+DSS mice was similar to
268 the community of the Broccoli mice, suggesting that broccoli sprouts strongly protected against
269 DSS-induced changes to the bacterial community (Figure 6A,B).

270 ***Beta dispersion.*** Mice in the Broccoli+DSS group had a bacterial community dispersion
271 (distance from centroids) larger than mice in the Control+DSS (Figure 6A,B), indicating more
272 heterogeneity in the bacterial communities between mice fed broccoli sprouts. The Broccoli and
273 Broccoli+DSS samples had a similar amount of dispersal between samples and the centroid for
274 these treatments (beta dispersion, $p > 0.05$ for both comparisons, adjusted with TukeyHSD for
275 multiple comparisons), indicating that broccoli sprouts negated any homogenization of the
276 bacterial community caused by DSS. The Control and Control+DSS communities do not overlap
277 and the Control+DSS community shows a tighter dispersal (beta dispersion, $p < 0.05$ for both
278 comparisons, adjusted with Tukey's HSD), indicating that DSS was a strong enough selective
279 pressure to reduce the individual variation of bacterial communities within the group.

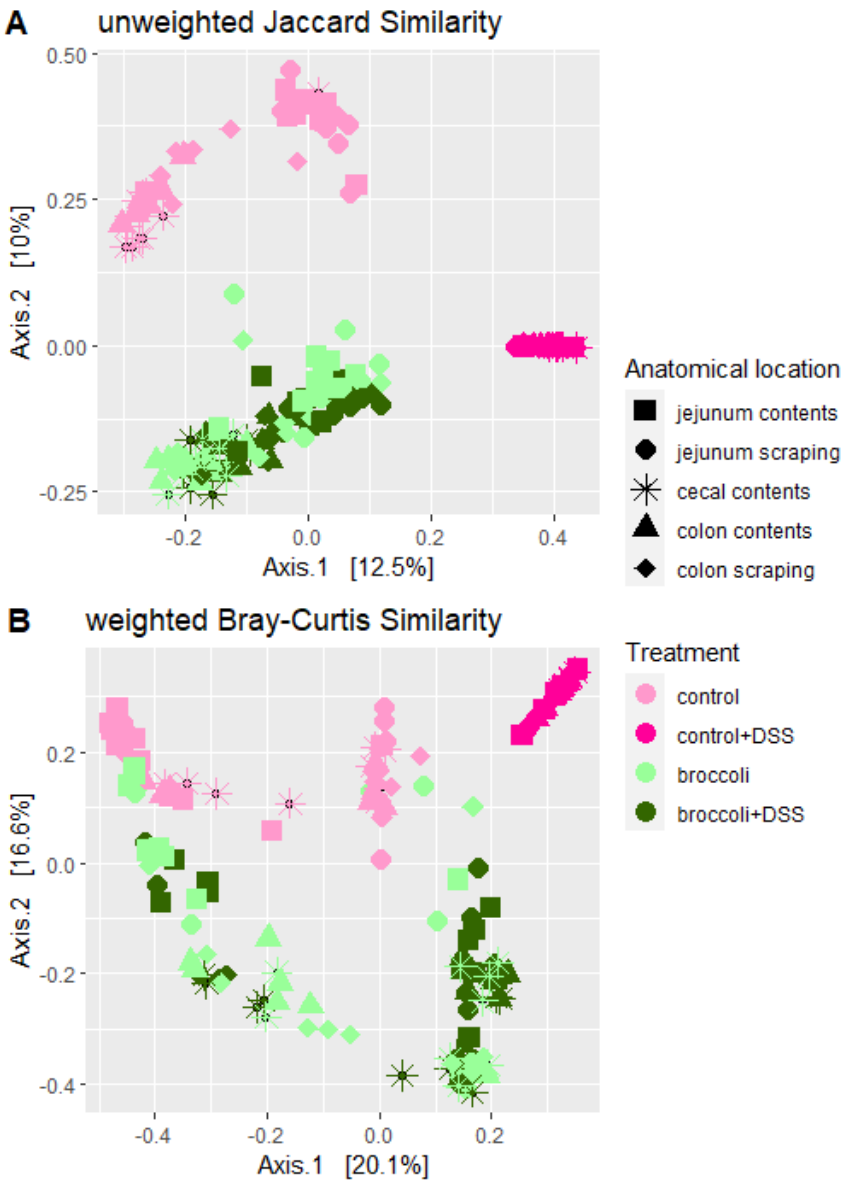

Figure 6. Principal coordinate analysis of bacterial community similarity along the intestines of mice under a DSS-induced model of chronic, relapsing colitis with or without 10% steamed broccoli sprouts in diet. Panel A was calculated with unweighted Jaccard Similarity to visualize differences in the taxonomic structure, and panel B with weighted Bray-Curtis to visualize structure and abundance.

Biogeography. Mice with induced colitis on the broccoli sprouts diet (Broccoli+DSS) indicated clustering associated with each anatomical location (jejunum contents & scrapings, cecal contents, colon contents & scrapings) whereas mice without broccoli sprouts did not

290 (Control+DSS, Figure 7A, permANOVA, uJS: $F = 3.42$, $p < 0.001$; wBC: $F = 4.36$, $p < 0.001$).
291 The variation within the Control+DSS group was obscured by the strong comparisons to other
292 groups in Figure 7A, so the Control+DSS samples were subset and demonstrated no biogeographic
293 clustering (Figure 7B, permANOVA, $p > 0.05$, except marginally between jejunum scrapings vs.
294 cecum contents, $p = 0.04$) when considering the bacterial community structure (unweighted
295 Jaccard Similarity; Figure 7B) or structure and abundance (weighted Bray-Curtis, not shown).
296

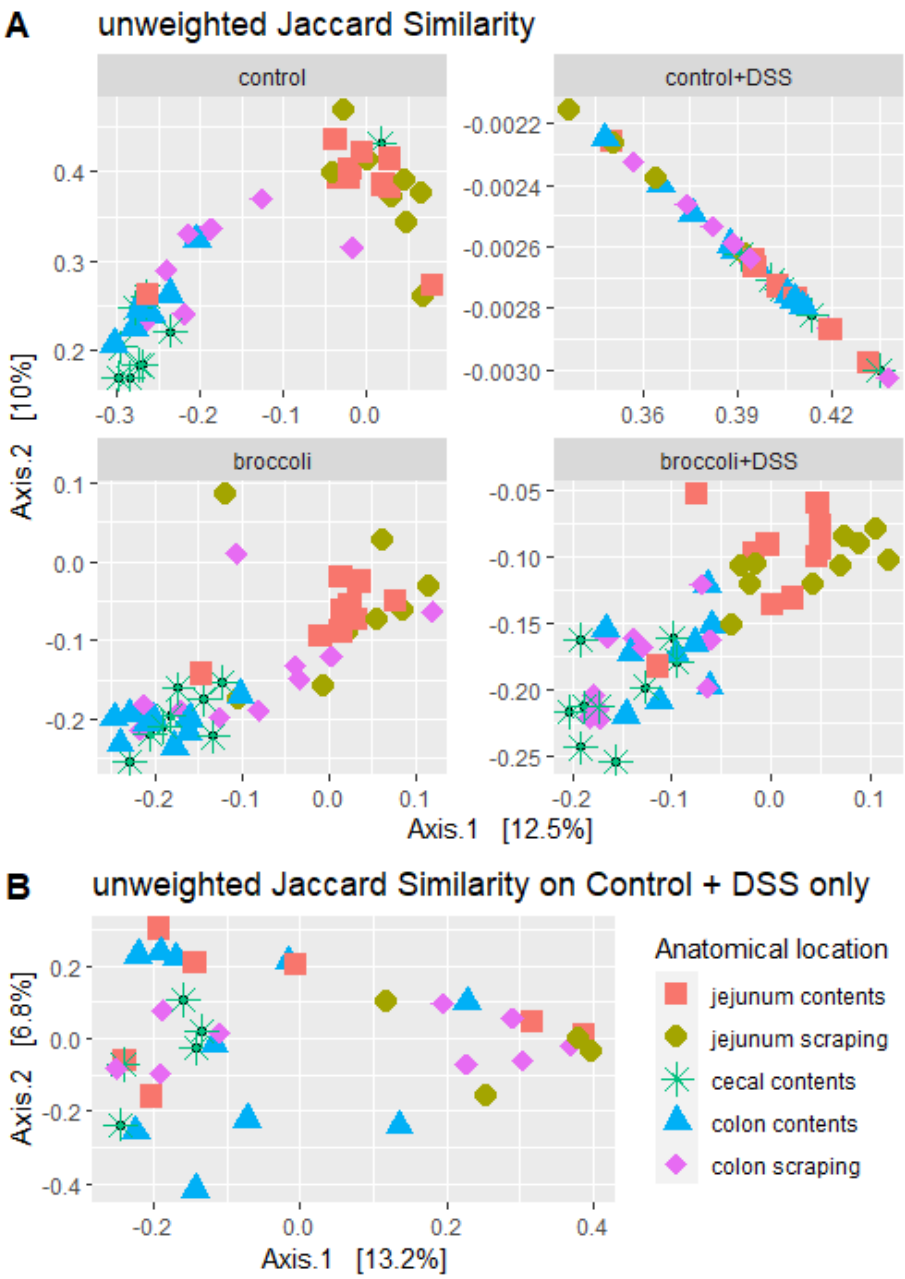

Figure 7. Principal coordinate analysis of bacterial communities from locations along the intestines of mice under a DSS-induced model of chronic, relapsing colitis with or without 10% steamed broccoli sprouts in diet: (A) All treatments (B) Control+DSS only. Bacterial communities in the jejunum, cecum, and colon were statistically different (permANOVA, $p < 0.05$) from each other in the treatment groups (A) Control, Broccoli, and Broccoli+DSS, were not statistically different from each other after multiple bouts of colitis in the (B) Control+DSS group.

306 ***Differential sequence variants.*** When identifying significant taxa which defined the
307 Control samples by anatomical location, there were 188 significant ($p < 0.05$) taxa identified, with
308 a permutational random forest model accuracy of 98% (Figure S2). Many of these defining taxa
309 in the Control mice were species considered to be mouse commensals, such as *Dubosiella* spp. and
310 strains from the Muribaculaceae and Lachnospiraceae families (Figure S2). The bacterial taxa
311 which defined the Control+DSS mice included the *Clostridium sensu stricto* clade, and fewer
312 commensal taxa were identified as important community members (Figure S3). The Broccoli
313 sprout group was differentiated by *Dubosiella* spp., *Parasutterella excrementihominis*, and
314 *Bacteroides* spp., among others (Figure S4). The Broccoli+DSS group had many of the same
315 important taxa as the group consuming Broccoli sprouts without colitis (Figure S5), implying a
316 strong selective pressure of the broccoli sprouts on the bacterial community structure. This was
317 supported by the identification of 'core taxa' which were present in high abundance across at least
318 70% of the Broccoli and Broccoli+DSS samples (Figure S6A). Similar to the differential SV
319 analysis, core bacteria in the Broccoli groups and core bacteria in the Control+DSS group did not
320 share many similar taxa (Figure S6B). There were no bacterial SVs which were shared across at
321 least 70% of samples in the Broccoli+DSS and the Control+DSS group (data not shown),
322 indicating there was not a specific community which was enriched or associated with the DSS.
323
324
325 **Taxa with putative GLR metabolism capacity present in broccoli sprout fed mice even**
326 **during colitis**
327 ***Putative glucoraphanin metabolizers.*** Mice with induced colitis on the broccoli sprouts
328 diet (Broccoli+DSS) indicated a dominant number of bacteria associated with the transformation

329 of glucoraphanin into sulforaphane and distinct from mice not on a broccoli sprout diet which had
330 relatively few (Control+DSS, Figure 8). The bacterial abundance in Broccoli+DSS mice was
331 greatly reduced in the colon contents and somewhat reduced in the cecum contents and colon
332 scrapings relative to the Broccoli mice. The bacterial abundance in Control+DSS mice increased
333 across all anatomical sites relative to the Control mice. There were 309 bacterial SVs identified in
334 samples to be associated with the expression of myrosinase-like enzymatic activity and the
335 transformation of glucoraphanin to sulforaphane, which represented the genera *Bifidobacterium,*
336 *Bacteroides, Enterococcus, Lactobacillus, Lactococcus, Pseudomonas, Staphylococcus,* and
337 *Streptomyces* (21, 43, 44) 29, 54, 55). No *Faecalibacterium*, *Bacillus, Listeria, Pediococcus,*
338 *Aerobacter, Citrobacter, Enterobacter, Escherichia, Salmonella, Paracolobactrum,* or *Proteus*
339 were found in the samples (Figure 8). *Bacteroides* were predominant in both the Broccoli+DSS
340 and Broccoli groups and much more abundant in comparison to all other genera across all samples
341 (1,394,934 frequency across all samples compared to a total frequency of 6,791 for all other
342 sequences; Figures 8,9).
343
344

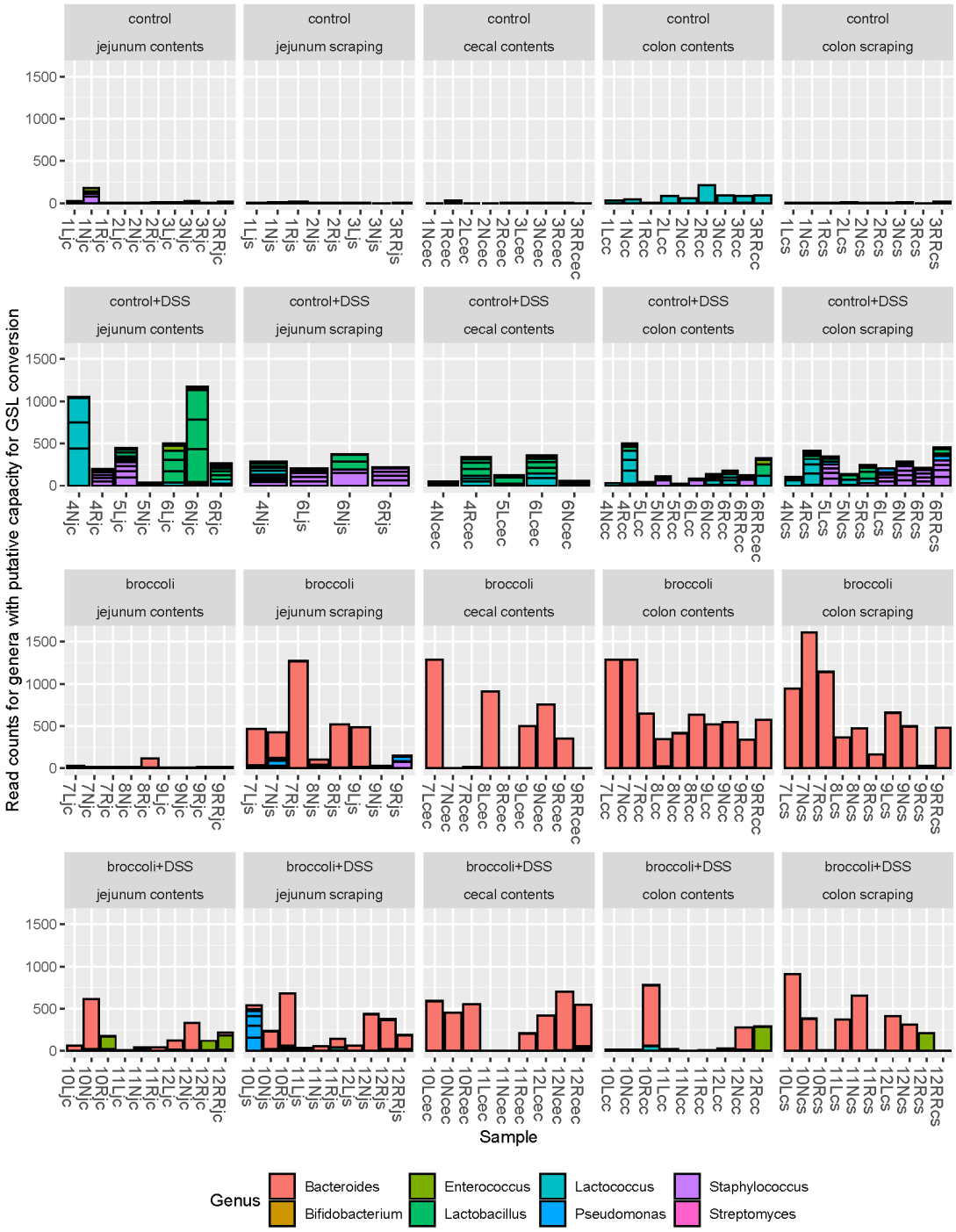

Figure 8. Bacterial sequence variants (SVs) belonging to the genera which have putative capacity to convert glucoraphanin to sulforaphane for mice under a DSS-induced model of chronic, relapsing colitis with or without 10% steamed broccoli sprouts in diet. Strains of bacteria in these genera have been demonstrated to perform myrosinase-like activity in the digestive tract, as reviewed in (43).

352 ***Bacteroides* species.** Several *Bacteroides* species were identified (*acidifaciens*,
353 *massiliensis*, *sartorii*), but the dominant sequence variant was not identified to the species-level
354 by the Silva Database taxonomy assignment (Figure 9A,B). This unidentified *Bacteroides*
355 dominant SV (*B.*-dominant) was associated with multiple species in the NCBI Database
356 (BLASTN): *Bacteroides thetaiotaomicron (B. theta)*, *Bacteroides faecis,* and *Bacteroides*
357 *zhangwenhongii,* all with 100% Query Cover and Percent Identity (Figure 9B). *Bacteroides theta*
358 has been linked to myrosinase-like enzyme activity (21), but *Bacteroides faecis* and *Bacteroides*
359 *zhangwenhongii* have not.

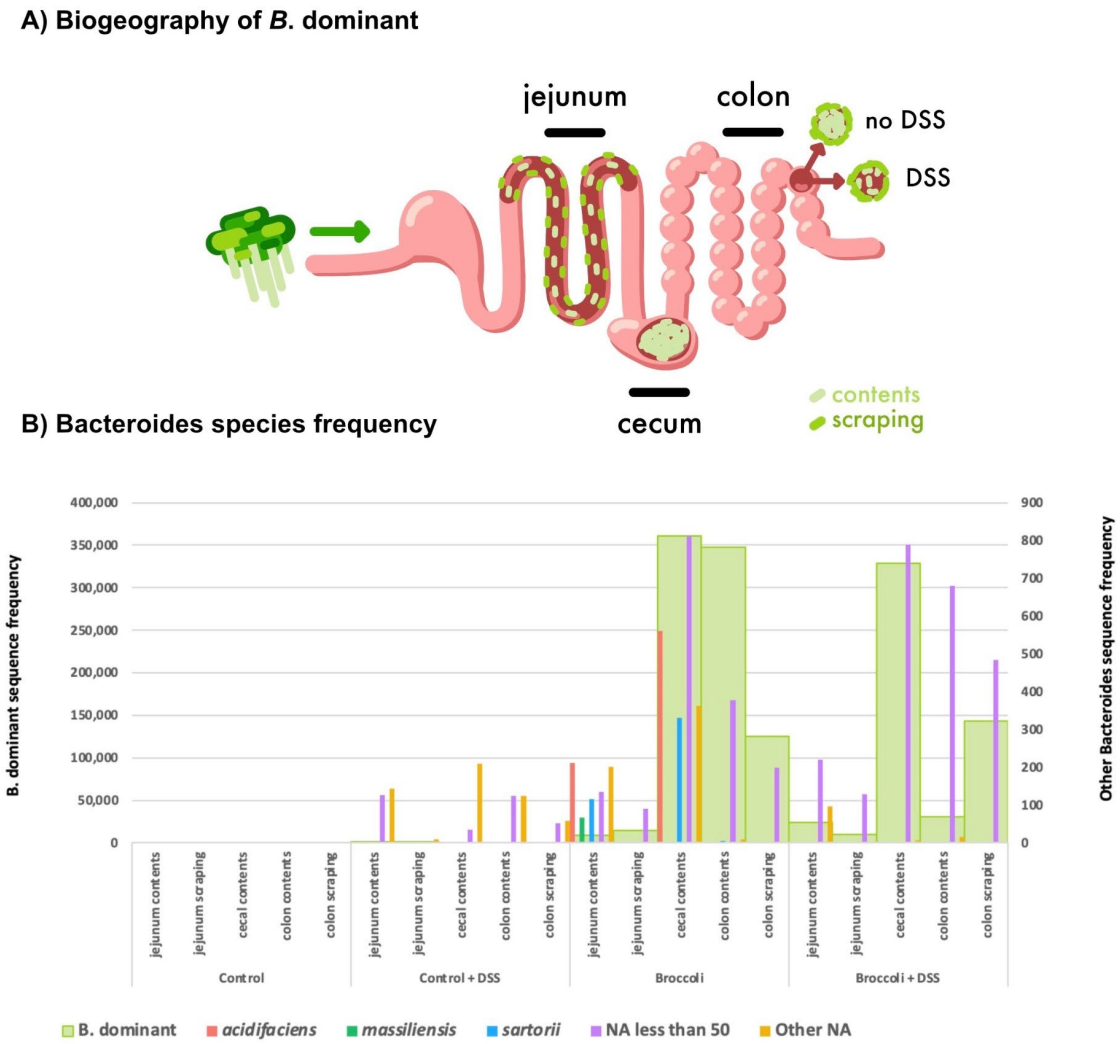

Figure 9. Biogeography of the dominant *Bacteroides* SV (*B.*-dominant) in the gut (A) and abundance of reads belonging to *Bacteroides* species by diet treatment and anatomical location in the gastrointestinal tract of mice. (A) *B.*-dominant was present in the jejunum contents and scrapings and abundant in the cecum contents, colon contents, and colon scrapings. DSS reduced *B.*-dominant colon content density. (B) The Silva Database identified *Bacteroides* species *acidifaciens*, *massiliensis*, and *sartorii*. Of the BLASTN identified species for *B.*-dominant SVs, only *B. thetaiotaomicron* was associated with broccoli-sprout-fed mice.

Bacteroides thetaiotaomicron (Bt VPI-5482). Amplification of bacterial genes via qPCR indicated the presence of the *B. thetaiotaomicron* operon BT2159-BT2156, responsible for glucoraphanin metabolism, along the digestive tract (Figure S7). In each of the anatomical sites,

373 BT2158 expression was most common followed by BT2157 and BT2156, BT2159, and then the
374 regulatory gene BT2160 (Figure S7). Copy numbers were not significantly different for any
375 individual gene by diet treatment and/or anatomical location (ANOVA, $p > 0.05$, adjusted for
376 multiple comparisons with TukeyHSD). However, the operon's GSL-metabolizing capacity is
377 highest when all four genes are present (21), thus we also assessed the presence of the operon
378 exhibited as collective gene copies, and samples demonstrated either high abundance (>100,000)
379 or low abundance (<100; Figure 10).

380 In the jejunum contents, 20% of Control mice had high presence of the operon BT2159-
381 2156 (Figure 10). By contrast, the Broccoli group had low presence of the operon, which was
382 associated with lower relative Bacteroidota (Figure S1), and the enrichment of SVs in the phyla
383 Firmicutes, Actinobacteriota, and Proteobacteria. This had resulted in higher ratios of average
384 Firmicutes/Bacteroidota (F/B: 72 v. 16), Actinobacteriota/Bacteroidota (A/B: 0.3 v. 0.1), and
385 Proteobacteria/Bacteroidota (P/B: 0.6 v. 0.3). Operon presence in the Control+DSS and
386 Broccoli+DSS jejunum contents was low. In the jejunum scrapings, more Control mice had a low
387 presence of the operon, while more Broccoli mice exhibited higher presence (Figure 10). In the
388 Control+DSS and Broccoli+DSS mice, the jejunum scrapings exhibited higher operon presence
389 relative to the jejunum contents (Figure 10).

390 In the cecum contents, the presence of all 5 genes in the Broccoli group shows an increase
391 in gene presence as compared to the jejunum samples in this group. Control+DSS and
392 Broccoli+DSS groups had higher presence of the operon than in the groups without DSS. The
393 operon presence in the Broccoli+DSS group is associated with *B.*-dominant and *Bacteroides* SVs
394 (Figure 9), but the Control+DSS increase is associated with large-scale changes to the bacterial
395 community (Figure S1): large reductions in Bacteroidota and Firmicutes, a large F/B ratio (118.5

396 v. 6.8), increased P/B (1.5 v. ~0), and a significant increase in Actinobacteriota (A/B = 10.16 v.
397 0.01). The cecum samples on a broccoli diet were associated with higher counts of Bacteroidetes,
398 Firmicutes, Actinobacteriota, and Proteobacteria and lower average ratios of F/B (10 v. 59), A/B
399 (0.068 v. 4.8), and P/B (0.31 v. 0.70) in the cecum compared to groups on the control diet.

400 The colon contents in the Control mice showed limited operon presence, with higher
401 abundance in scrapings, while the Control+DSS mice had higher operon presence in both the colon
402 sites (Figure 10). The Broccoli mice showed higher operon presence in the contents as compared
403 to the scrapings, while the Broccoli+DSS group had the opposite pattern.

	Contents			Scrapings	
Treatment	Jejunum	Cecum	Colon	Jejunum	Colon
Control	70%	67%	90%	80%	70%
	10%	22%	0%	10%	10%
	20%	11%	10%	10%	20%
Broccoli	89%	50%	67%	90%	80%
	11%	30%	11%	0%	10%
	0%	20%	22%	10%	10%
Ccontrol+DSS	89%	75%	50%	67%	63%
	11%	0%	30%	11%	0%
	0%	25%	20%	22%	38%
Broccoli+DSS	90%	70%	60%	80%	80%
	0%	0%	30%	10%	0%
	10%	30%	10%	10%	20%

BT2159-BT2156 operon		
Mean copy number		
0%	0%	0%
10%	10%	10%
20%	20%	20%
30%	30%	30%
40%	40%	40%
50%	50%	50%
60%	60%	60%
70%	70%	70%
80%	80%	80%
90%	90%	90%
100%	100%	100%
Low		High
<100		>100,000

404
405 **Figure 10: Prevalence of the operon BT2159-BT2156 in *Bacteroides thetaiotaomicron* (VPI-**
406 **5482) in mice with and without chronic, relapsing DSS-induced colitis where diet was**
407 **manipulated.** Percentages are based on the number of samples (by diet and anatomical location)
408 in each category of gene abundance (minimum mean copy numbers: red low <100, purple medium
409 100-100,000, blue high >100,000) across all 5 genes in the operon.
410
411
412 **Discussion**

413 **Broccoli sprouts protected mice against DSS-induced colitis**

414 The anti-inflammatory effects of broccoli and broccoli sprout bioactives, in particular
415 sulforaphane (SFN), have been well-established in various cell, animal, and human trials of IBD

416 (17). However, studies have not elucidated the role of the whole gut communities, or patterns of
417 biogeography, on the capacity of bacteria to metabolize the glucoraphanin (GLR) precursor to
418 SFN. Juvenile SPF C57BL/6 mice (7-11 weeks) were fed a diet featuring 10% steamed broccoli
419 sprouts, which was balanced by macronutrients and fiber, and which contained glucoraphanin but
420 no plant myrosinase, thus gut microbiota were solely responsible for any production of the anti-
421 inflammatory sulforaphane. Under chronic, relapsing DSS-induced colitis (3 cycle regime), the
422 steamed broccoli sprout diet group demonstrated mitigated weight loss; reduced Disease Activity
423 Index, plasma lipocalin, and proinflammatory cytokines; the presence of bacterial taxa which are
424 known to metabolize GLR to SFN; and retained biogeographical patterns of bacterial communities
425 in different locations in the gut. Moreover, broccoli sprouts reduced the occurrence of fecal blood,
426 which is known to increase the abundance of pathobionts and reduce commensals (45, 46).

427 Lipocalin is a neutrophil protein produced by epithelial cells and secreted luminally and
428 through intestinal tissue where it is absorbed into the blood (47), and serves as a surrogate marker
429 for intestinal inflammation in IBD (47). Plasma lipocalin was high in our Control+DSS mice, but
430 low for the Broccoli+DSS diet which suggests that broccoli sprouts prevented severe physical
431 destruction of the epithelium. Similarly, the lower concentration of plasma cytokines in the
432 Broccoli+DSS mice indicates a lower innate immune response, and which may be the result of an
433 intact epithelial barrier that prevented bacterial translocation from the lumen to intestinal tissues
434 (34).

435 Broccoli sprout feeding was initiated before the introduction of DSS. This was done partly
436 to acclimate mice to the diet, but primarily to investigate the efficacy of broccoli sprouts as a
437 prevention strategy before initiating colitis. Previous studies have demonstrated its usefulness in
438 alleviating symptoms during active disease states (13). To validate the feasibility of broccoli as a
439 treatment for DSS-induced colitis, a 10% steamed broccoli sprout diet was used with male mice,

440 as they are known to suffer more histopathological damage from DSS-induced colitis (48, 49).
441 Regular access to fiber is critical to recruiting and retaining beneficial microbiota in the gut (50),
442 and regular exposure to glucosinolates is needed to stimulate gut microbial conversion of GLR to
443 SFN (51). In individuals who sporadically consume broccoli or broccoli sprouts, or consume them
444 over short periods of time, the cooking preparation and the activity/inactivity of plant myrosinase
445 were often the determining factors in the production of SFN, if any (51). However, directly
446 including SFN in the diet is not feasible due to its instability (24). This approach would also hinder
447 the potential for other benefits and the overall enjoyment of consuming a food rich in phenols and
448 fiber.

449 We acknowledge that a major limitation in this study was only using male mice, as it is
450 known that hormones mediate both the gut microbiome and the type and intensity of DSS-induced
451 colitis. Thus, any future research on the application of this diet in people will require diversity in
452 the gender of participants.

453

454 **Bacterial communities are highly responsive to DSS and broccoli sprouts**

455 The broccoli sprout diet increased bacterial richness, regardless of DSS treatment, and as
456 the control and sprout diets were balanced for total fiber it is likely that fiber was not solely
457 responsible for this effect. In particular, broccoli sprouts increased bacterial richness in the colon.
458 We previously showed that the concentration of SFN is highest in the colon after feeding C57BL/6
459 mice steamed broccoli sprout diets which has reduced myrosinase concentrations, suggesting that
460 primary hydrolysis of SFN to GLR by microbial communities occurs in the colon (32). The current
461 study found effects on microbial richness from the broccoli sprout diet manifested most strongly
462 in the colon, supporting our previous findings.

463 When identifying significant taxa which defined the samples in different treatments, the
464 Control mice contained a high abundance of known mouse commensal taxa, including *Dubosiella*
465 spp. and strains from the Muribaculaceae and Lachnospiraceae families. The Control+DSS mice
466 contained much lower abundance of known mouse commensal taxa and higher abundance of the
467 *Clostridium sensu stricto* clade (52), which contains known pathogens such as *Clostridium*
468 *perfringens* (53), and well-known butyrate-producing symbionts, such as *Clostridium butyricum*
469 (54).

470 The Broccoli sprout group was also high in commensal taxa such as *Dubosiella* spp., and
471 had enrichment of *Bacteroides* spp., a genus known to contain glucosinolate-metabolizing bacteria
472 and modified by cruciferous vegetable consumption (55). The broccoli sprout diet enriched for
473 *Parasutterella excrementihominis* in the gut, which is commonly found in human and murine gut
474 communities and is associated with carbohydrate intake (56). It is possible that other breakdown
475 products of glucosinolates, such as aromatic carbohydrate compounds in broccoli sprouts (57),
476 caused this enrichment (57). *Parasutterella excrementihominis* has also been associated with
477 inflammation in the gut in observation-based studies; however in metabolic pathway-based studies
478 it appears to be an important contributor to nitrate reduction in the gut and in reducing stress-
479 related inflammation (58). Nitrates are low in raw broccoli and other cruciferous vegetables, but
480 this can be increased by freezing (59). Thus, our diet preparation – which included freezing and
481 freeze-drying steps – may have selected for nitrate-reducers. Also, outside of the mucosa, SFN has
482 an anti-bacterial effect (17), which may explain why putative pathogenic genera were lower in
483 Broccoli groups as compared to the Control+DSS group.

484 Importantly, the Broccoli+DSS group had many of the same important taxa as the group
485 consuming Broccoli sprouts without colitis, implying that the selective pressure of the broccoli

486 sprouts on the bacterial community structure may be stronger than that of the DSS. The two
487 treatments were so similar that many SVs were found in high abundance across at least 70% of the
488 samples in those mice. There were no bacterial SVs shared across at least 70% of the
489 Broccoli+DSS and the Control+DSS group, indicating there was not a specific community which
490 was enriched or associated with the DSS.

491 The inclusion of DSS in drinking water demonstrably affects mice and gut bacterial
492 communities, but it does not necessarily reduce bacterial richness. Control+DSS mice hosted more
493 bacterial richness than Control mice in the jejunum, and similar richness in the colon, although the
494 distinct ordination clustering between Control and Control+DSS samples indicates different
495 communities present regardless of similar richness, and the tight grouping of the Control+DSS
496 community indicates a strong selective pressure. In part, Control+DSS mice may retain gut
497 richness because certain bacteria, like *Proteus vulgaris,* can make use of DSS (60), while other
498 novel commensals, like some *Bacteroides*, appear to offer protective effects (61). We did not
499 identify any bacterial SVs belonging to *Proteus*, although we found significantly higher amounts
500 of *Bacteroides* sp. in broccoli sprout-fed mice. *Bacteroides thetaiotaomicron* has been
501 demonstrated to metabolize glucoraphanin to sulforaphane and offer protection against colitis in
502 mice (21).

503 Across multiple mouse lineages, individualized bacterial communities responded
504 differently to the inclusion of DSS, and the presence of *Duncaniella muricolitica* and *Alistipes*
505 *okayasuensis* were implicated in better mouse health outcomes (62). Modeling of the gut
506 microbiome indicates that certain taxa may act as keystone species – critical to building the rest of
507 the community and particularly in circumstances in which the microbial community has been
508 destabilized (63). However, no single important bacterial taxa has been identified in meta analyses

509 of IBD in humans (64, 65), and some studies have pointed to the switch of bacterial commensals
510 to acting as pathobionts as important (66).

511 There is considerable evidence that microbes provide metabolism of biologically inert
512 glucosinolates to biologically active isothiocyanates, and several cultured bacterial strains from
513 fermented foods and the digestive tract have been shown to perform this conversion (21, 43, 44).
514 Additionally, a single bacterial equivalent of the plant myrosinase enzyme has not been identified,
515 and there is the possibility that several enzymes in bacteria may work in concert to achieve
516 metabolism of GSLs. Further, research is lacking to determine if the effect on the gut microbiome
517 is metabolite (isothiocyanates)-mediated or precursor (glucosinolates)-mediated. The scope of
518 research in this field should be expanded by investigating the concepts of biogeographic specificity
519 of both bioactive production and absorption and microbial community dynamics.
520

521 **Biogeography reveals location-specific trends in bacterial communities**

522 It has been well-demonstrated that distinct bacterial communities exist in different
523 locations along the gastrointestinal tract in mammals, related to the local anatomical,
524 environmental, nutritional, and host immunological conditions in different organs (67–69).
525 Further, the effect of foods on the gut microbiome can be specific to an individual's communities
526 (27). Given the complexity of microbial community function, as well as the spatially explicit
527 biochemical digestion activities of the host, it follows that the location of glucoraphanin
528 metabolism may influence how well the host can absorb SFN, whether it may be distributed
529 systematically, and where it will be effective at preventing or treating symptoms. It has previously
530 been demonstrated in mouse trials using 2,4,6 trinitrobenzene sulfonic acid to chemically induce

531 colitis that the mucosal-associated bacterial population is more affected by colitis than the lumen-
532 associated (digesta) community (36).

533 Here, we showed that DSS-induced colitis effectively erased the biogeographical
534 specificity of communities in the mouse gastrointestinal tract, with the exception of communities
535 in jejunum scrapings remaining distinct from those in cecal contents. Given the highly specific
536 function of the cecum in separating fibers by size and furthering microbial fermentation, it is not
537 surprising that it would be distinct. We sampled the jejunum because it is not often reported on in
538 IBD studies, and does not always show effects of inflammation. We confirmed that bacteria in the
539 jejunum are negatively affected by DSS. The DSS may be a stronger selective force than
540 anatomical location in driving bacterial communities in the gut (61). For example, its destruction
541 of the epithelial cell surface may change the microarchitecture and alter microbial attachment in
542 the gut (70), and DSS increases the hydrophobicity of bile acids (71), which may affect microbial
543 survival and ability to attach to host epithelial cells, thus increasing microbial washout through the
544 gut. Any of these could possibly explain our findings that DSS eliminated biogeographical
545 specificity of communities in the mouse gastrointestinal tract. However, more research would be
546 needed to determine causation.

547 Mouse studies suggest biotransformation of glucoraphanin to SFN occurs in the colon (21,
548 25, 26), and we previously confirmed the majority of SFN accumulation takes place in the colon,
549 with greater resolution using multiple locations along the GI tract (13). Critically, the cecum had
550 low SFN, indicating that it is not responsible for hosting bacterial biotransformation of these
551 bioactives (13). Here, we also showed that only a few bacterial taxa were estimated to be sourced
552 in the cecum and creating sink populations in the colon, and of these, none were identified to be

553 putatively responsible for metabolism of glucoraphanin. Collectively, this confirms that this is a
554 valid model for generalization to the human gut.
555

556 **Putative GLR-metabolizers more abundant in sprout diets, but gene copies were not**
557 **uniformly increased**

558 Comparative analysis of the BLAST identification of SVs and qPCR of the gene copies in
559 the operon BT2160-2156 suggest that the dominant Bacteroides SV identified by 16S rRNA
560 sequencing largely represents *B. thetaiotaomicron*. The Broccoli diet (no DSS) induced the
561 presence of *B.*-dominant in the jejunum contents and scrapings, and more so in the cecum contents
562 and the colon contents and scrapings. The addition of DSS (Broccoli+DSS) noticeably reduced *B.*-
563 dominant in the colon contents although it was maintained in the cecum and colon scrapings.
564 Importantly, the results presented here used only DNA from viable cells, but not RNA, and it is
565 known that *Bacteroides* and particularly *B. theta* exhibit highly situational carbohydrate and glycan
566 digestion. Thus, the presence of *B. theta* or other putative GLR-metabolizers does not confirm
567 their activity, which may explain why these taxa and GLR-metabolizing genes were also present
568 in the Control and Control+DSS in low abundance.
569 Whereas the lumen (contents) may represent a transient view of a gut bacterial community,
570 the mucosal-associated populations (scrapings) are more resistant to short-term changes to the diet
571 or gut ecosystem. There was no *B.*-dominant present in the Control group's jejunum contents or
572 scrapings after 34 days of trial, but there were genes copies of the *B. theta* GLR-metabolizing
573 operon, which suggests that gene copies were from the many unclassified Bacteroidota or
574 *Bacteroides* SVs in the jejunum contents and scrapings sequencing samples, or from other genera
575 containing an operon orthologous to BT2159-BT2156. By contrast, the Broccoli groups's jejunum

576 contents and scrapings include *B.*-dominant, with considerably higher frequencies in the scrapings,
577 as well as higher prevalence of all 5 genes in the operon. This is further demonstrated in the DSS
578 groups for both diets, in which the jejunum scrapings demonstrated higher prevalence of all 5
579 genes in the operon relative to the jejunum contents. Interestingly, the Control+DSS group had
580 twice the prevalence of high copy numbers across all 5 genes, but no B.-dominant SVs, again
581 suggesting the existence of the genes was due to other unclassified Bacteroidota or *Bacteroides*.

582 As chime flows from the jejunum to the cecum, it enters the less hostile (neutral to slightly
583 alkaline) and primary fermentation environment of the cecum, where the bacterial density typically
584 increases by orders of magnitude in healthy animals. In our samples, higher abundance of the
585 operon was found in the cecum, as GLR-metabolizers are possibly benefiting from its slower
586 transit time and more favorable fermentation environment. The presence of all 5 genes in the
587 Broccoli group shows a dramatic increase in gene presence, as well as *B.*-dominant and
588 *Bacteroides* SVs, as compared to the jejunum samples in this group. Interestingly, in the DSS
589 groups for both diets, the prevalence of gene copies in the operon is higher than in the groups
590 without DSS. The increase in the Broccoli+DSS group is associated with increased *B.*-dominant
591 and *Bacteroides* SVs, but the Control+DSS increase is associated with phylum-scale changes to
592 the bacterial community.

593 The Control and Control+DSS colon contents contained limited operon presence, with only
594 slightly higher abundance in scrapings, and are largely absent of *B.*-dominant. The Broccoli and
595 Broccoli+DSS groups contained more operon in the colon contents than the scrapings. In the colon
596 contents in both broccoli sprout groups, *B.*-dominant was identified in a few mice, but *Bacteroides*
597 counts were much higher and were not impacted by the DSS treatment. In the colon scrapings in
598 both broccoli sprout groups, *B.*-dominant was more prevalent and dominant, suggesting the

599 possibility of *B*.-dominant GLR-metabolism in the mucosal-associated sites, and other *Bacteroides*
600 providing GLR-metabolism in the Broccoli+DSS colon contents.
601
602
603

604 **Considerations for the application of this work**

605 Access to fresh or frozen broccoli and broccoli sprouts, the cooking preparation, and the
606 ability to regularly consume these vegetables will have implications for the feasibility and success
607 of a dietary intervention for preventing or reducing inflammation in the gut. For example, sprouts
608 from various plants have been implicated in food-borne illness because of their proximity to soil,
609 and people may be wary of or discouraged from consuming raw or slightly cooked sprouts.
610 However, more recent research has shown that sprouts can be consumed safely, especially with
611 improvements in hygiene and agricultural regulations, as well as in food processing (72). Further,
612 broccoli sprouts can be grown at home in windowsill seed-bed germinators without requiring soil,
613 gardening tools, or specialized gardening knowledge, which could ease the financial burden of
614 purchasing healthy foods (73). This may prove to be particularly important in areas without access
615 to healthcare or affordable prescriptions, or in areas without close proximity to fresh, healthy fruits
616 and vegetables (5, 74, 75) as this can preclude being able to make the dietary recommendations
617 set forth by medical professionals (76). Including broccoli sprouts as 10% of the diet could be
618 potentially too high for IBD patients to comply with, and future studies on the application of this
619 diet will require a deeper understanding of the biological, microbiological, immunological, as well
620 as social and logistical factors involved in dietary interventions in people.
621
622

623 **Materials and Methods**

624 **Diet preparation**

625 Jonathan's Sprouts™ (Rochester, Massachusetts, USA) broccoli sprouts were purchased
626 from a grocery store (Bangor, Maine, USA) and steamed in a double boiler for 10 minutes,
627 immediately cooled down, and stored in a -80°C freezer until freeze-drying (University of Maine
628 Food Pilot Plant, Orono, Maine, USA). The freeze-dried broccoli sprouts were ground into a fine
629 powder and mixed with purified AIN93G rodent base diet (Envigo, now Inotiv, Indianapolis,
630 Indiana, USA) to a concentration of 10% by weight. The AIN93G diet contains 50 g/kg of fiber as
631 cellulose (77), and broccoli sprouts contain 35 g/kg fiber, thus the broccoli sprout-fed mice
632 consumed a similar amount of fiber on a per weight basis. The diets were measured to balance
633 their weight prior to feedings; however, we did not measure food intake or refusals. Anecdotal
634 animal care notes and visual observation of cages across multiple previous studies indicate that
635 control and broccoli sprout groups do not consume different amounts of food (Li and Ishaq,
636 personal communications.

637 Our previous work assessed the effects of different diet preparations and the percentage of
638 broccoli sprouts, and found that 5-10% broccoli sprouts by weight reliably produces consistent
639 anti-inflammatory results in mice (13). For this study, we chose to use 10% steamed broccoli
640 sprouts both to assess the microbial conversion of GLR to SFN, and to ensure that the intervention
641 would have a strong effect (48, 49, 78). Diet pellets were formed using a silicone mold to ensure
642 consistent sizing, and allowed to dry at room temperature for up to 48 hours in a chemical safety
643 hood to facilitate moisture evaporation, and after drying were stored in sealable plastic bags in a -
644 20°C freezer.

645

646 **DSS colitis model**

647 The dextran sodium sulfate (DSS) mouse model is widely used to study human Ulcerative
648 Colitis (UC) (41, 79), and has been used for studying diet-sourced anti-inflammatories for the
649 prevention of IBD (40, 41). Administration of DSS in drinking water modifies the expression of
650 tight junction proteins in intestinal epithelial cells, leading to a leaky epithelial barrier (80). This
651 is followed by goblet cell depletion, erosion, ulceration, and infiltration of neutrophils into the
652 lamina propria and submucosa (81), triggering the innate immune response (82, 83).

653 Forty male, 6-week-old, specific pathogen free (SPF) C57BL/6 mice (*Mus musculus*) were
654 purchased from the Jackson Laboratory (Bar Harbor, Maine, U.S.) and transferred to the animal
655 facility at the University of Maine (Orono, Maine, U.S.). The animal protocol (IACUC protocol
656 A2020-01-04) was approved by the University Committee on the Use and Care of Animals, and
657 all biosafety work was approved by the Institutional Biosafety Committee (protocol SI-092220).
658 The mice were acclimated to the facility for 7 days (day -6 to 0), during which they received *ad*
659 *libitum* autoclaved tap water and the AIN-93G purified rodent diet (control diet). After initial
660 acclimation, the mice were randomly assigned to one of 4 experimental groups beginning on
661 experimental day 1: control diet without DSS treatment (Control), 10% steamed broccoli sprout
662 diet without DSS treatment (Broccoli), control diet with DSS treatment (Control+DSS), and 10%
663 steamed broccoli sprout diet with DSS treatment (Broccoli+DSS). All experimental groups were
664 on 7 days of their respective diets (control or 10% steamed broccoli sprout), after which DSS (Alfa
665 Aesar, molecular weight ~40 kD (39)) was added to the drinking water of the DSS treatment
666 groups to a final concentration of 2.5%. Mice were given DSS for 5 days, followed by a recovery
667 period for 5 - 7 days. This was repeated for a total of 3 cycles to induce chronic colitis (40, 84).
668 Mice were sacrificed and tissue collected after the third round of DSS, on day 35 of the experiment.

669 Bodyweight, fecal blood, and fecal consistency were used to calculate Disease Activity
670 Index (DAI) scores (83). Fecal samples were collected every 2 - 3 days throughout the trial, and
671 daily during the DSS cycles. Body weights and DAI were analyzed using 2-way ANOVA
672 generated with R to compare differences between treatments for each day. A generalized additive
673 model (GAM) was used in R to compare DAI differences (R-sq.(adj) = 0.861, Deviance explained
674 = 86.4%, GCV = 0.036031) by treatment across the entire study, using Mouse ID to account for
675 repeated measures.

676 Lipocalin-2 concentration in the plasma samples were determined by a mouse Lipocalin-
677 2/NGAL DuoSet ELISA kit (R & D Biosystems, USA) following the manufacturer's instructions.
678 Lipocalin is a neutrophil protein that binds bacterial siderophores and serves as a surrogate marker
679 for intestinal inflammation in IBD (47). The readings at wavelengths of 540 nm and 450 nm were
680 measured by a Thermo Scientific Varioskan LUX Multimode Microplate Reader. The readings at
681 540 nm were subtracted from the readings at 450 nm to correct for the discoloration of the solution.
682 ANOVA was used to compare lipocalin values.

683 We analyzed several cytokines in the mouse plasma samples which were collected at the
684 end of the study. CCL4, also known as macrophage inflammatory protein 1β (MIP1β), is a
685 chemokine that plays a critical role in regulating the migration and activation of immune cells
686 during inflammatory processes (42). Interleukins IL-1β and IL-6; and tumor necrosis factor alpha
687 (TNF-α) are pro-inflammatory cytokines that play key roles in the regulation of the immune
688 response (85–87). The concentrations of mouse CCL4/MIP-1β, IL-1β/IL1F2, IL6, and TNF-a were
689 analyzed using the Simple Plex Ella Automated Immunoassay System (Ella) from R&D
690 Biosystems, USA. Mouse serum samples were diluted 10-fold using the reagent diluent provided
691 with the kit (SPCKA-MP-007374, Protein Simple, Bio-Techne), and the concentrations were

692 determined following the manufacturer's instructions. The Ella system was used to perform the
693 immunoassay, and mean values were calculated for each analyte. The resulting data were used for
694 statistical analyses using ANOVA.

695 After euthanasia, lumen-associated (digesta contents) and mucosal-associated (epithelial
696 scrapings) microbial community samples were collected from the jejunum, cecum (contents only),
697 and colon for DNA extraction, gene quantification, and community sequencing as described
698 below.

699

700 **Bacterial community sequencing and analysis**

701 Immediately following euthanasia of the mice, digesta (lumen contents) and epithelial
702 associated (tissue scrapings) microbial community samples were collected from the jejunum, the
703 cecum (contents only), and along the entire colon, as the inflamed mice had short colons and
704 limited amounts of digesta present. All samples of gut microbiota were gently homogenized with
705 vortexing, then treated with propidium monoazide (PMA; BioTium) following kit protocols at a
706 final concentration of 25 μm. PMA covalently binds to relic/free DNA and DNA inside
707 compromised/dead cell membranes, and prevents amplification in downstream protocols to
708 preclude dead DNA from the sequence data (88).

709 Following PMA treatment, bulk DNA was extracted from bacterial communities (n = 200
710 samples), or no-template (water) control samples (n = 10, one for each extraction batch) using
711 commercially available kits optimized for water and tissue-based microbial communities (Quick-
712 DNA Fecal/Soil Kit, Zymo Research). DNA extract was roughly quantified and purity-checked
713 with a Thermo Scientific™ NanoDrop™ OneC Microvolume UV-Vis Spectrophotometer
714 (Thermo Scientific, Waltham, MA, U.S.). Samples underwent DNA amplicon sequencing of the

715 16S rRNA gene V3-V4 region, using primers 341F and 806R and protocols consistent with The
716 Earth Microbiome Project (89), and sequenced on an Illumina MiSeq platform using the 2 x 300-
717 nt V3 kit (Molecular Research Labs, Clearwater, TX, U.S.). Raw sequence data (fastq files and
718 metadata) is available from NCBI through BioProject Accession number PRJNA911821.

719 Amplicon sequence data was processed using previously curated workflows in the Ishaq
720 Lab (R code supplied as Supplemental Material), which used the DADA2 pipeline ver. 1.26 (90)
721 in the R software environment ver. 4.1.1 (91). The dataset started with 46,581,832 paired raw
722 reads, and based on initial quality assessment only the forward reads were processed. Trimming
723 parameters were designated based on visual assessment of the aggregated quality scores at each
724 base from all samples (plotQualityProfile in DADA2): the first 10 bases were trimmed, sequences
725 were trimmed to 225 bases in length, and were discarded if they had ambiguous bases, more than
726 two errors, or matched the PhiX version 3 positive control (Illumina; FC-110-3001). After
727 filtering, 34,009,802 non-unique forward/read 1 sequences remained.

728 The DADA algorithm was used to estimate the error rates for the sequencing run,
729 dereplicate the reads, pick sequence variants (SVs) which represent 'microbial individuals', and
730 remove chimeric artifacts from the sequence table. Taxonomy was assigned using the Silva
731 taxonomic training data version 138.1 (92) down to species where possible, and reads matching
732 chloroplasts and mitochondria taxa were removed using the dplyr package (93). No-template
733 control samples were used to remove contaminating sequences from the samples by extraction
734 batch (94). The sequence table, taxonomy, and metadata were combined for each experiment using
735 the phyloseq package (95), which was also used for basic visualization and statistical analysis in
736 combination with other packages. Samples from one mouse (4L, in the Control+DSS group) were

737 dropped from further analysis as they were outliers on all visualizations and may have been
738 contaminated during DNA extraction.

739 Normality was checked using a Shapiro-Wilkes test on alpha diversity metrics generated
740 from rarefied data, including observed richness, evenness, and Shannon diversity. Linear models
741 were run for comparisons of alpha diversity metrics to compare by sample type, (lme4 package
742 (96)), in which anatomical location and diet treatment were used as fixed effects, and mouse ID
743 used to control for repeated sampling as needed. Generalized additive models were used to assess
744 trends in alpha diversity using time as a smoother (97). Jaccard unweighted similarity was used to
745 calculate sample similarity based on community membership (species presence/absence),
746 visualized with non-parametric multidimensional scaling, and tested with permutational analysis
747 of variance (permANOVA) by using the vegan package (98). Random forest feature prediction
748 with permutation was used to identify differentially abundant SVs based on factorial conditions
749 (99). Plots were made using the ggplot2 (100), ggpubr (101), and phyloseq packages.

750 Source Tracker algorithms which had been modified for the R platform (102, 103) were
751 used to identify source:sink effects based on anatomical location. This was used to determine if
752 the cecum could be the source for population sinks in the colon, as a proxy for the model's
753 applicability to the human gut anatomical features and microbial communities. A total of 142 SVs
754 were identified as possibly sourced from the cecum, and 95 SVs were estimated to make up >1%
755 of the proportion of sources (Figure S8). The putative GLR converting bacteria in the Broccoli and
756 Broccoli+DSS mouse gut samples were not among those taxa identified as sourced in the cecum.

757

758 **Quantitative PCR for glucoraphanin metabolism genes**

759 DNA extract from all gut locations was used to assess microbial potential for glucoraphanin
760 conversion. Bacterial genes, gene sequences, and primers associated with conversion of GSLs to
761 ITCs identified in *Bacteroides thetaiotaomicron* VPI-5482 (21) were used, and are listed in Table
762 S1. These primers were evaluated for validity using IDT's OligoAnalyzer (www.idtdna.com) and
763 NCBI primer blast (https://www.ncbi.nlm.nih.gov/tools/primer-blast/). The identified genes from
764 *Bacteroides thetaiotaomicron* VPI-5482 were analyzed by using the ApE-A plasmid Editor v3.1.3
765 to optimize and validate the primers for optimal GC content and melting temperature.

766 Quantitative polymerase chain reaction (qPCR) was performed on extracted DNA using
767 the Applied Biosystems QuantStudio 6 Flex Real-Time PCR system (Applied Biosystems, Foster
768 City, CA, USA). Luna® Universal qPCR Master Mix and primer sets BT2156-BT2160 were used
769 to quantify copy numbers of glucoraphanin-metabolizing genes previously identified from
770 *Bacteroides thetaiotaomicron*. Primers were diluted to 10 μM, for a final concentration of 0.25
771 μM in each well. Each primer set required one cycle of 50°C for 2 min, one cycle of 95°C for 1
772 min, and forty cycles of 95°C for 15 sec, 60°C for 30 sec and 72°C at either 20, 25 or 30 sec
773 depending on the primer set. A standard curve for each gene was created using a set of 7 serially
774 diluted geneblocks (IDT). All samples and standards were run in triplicate, across two 384-well
775 plates with negative controls and standards included on both plates. Primer sequences, geneblock
776 sequences for standards, and protocols are listed in Table S1. Sample gene copy numbers were
777 calculated using the standard curve in the Quantstudio analysis software. Data were visualized and
778 statistically analyzed in R using analysis of variance models corrected for multiple comparisons

using Tukey's HSD. Similar to the bacterial community data, sample 4L was dropped from the qPCR data analysis as an outlier/possible contamination.

Acknowledgements

All authors have read and approved the final manuscript. The authors thank Jess Majors, University of Maine, for her kind and detailed care of the mice during the trial, and for Ellie Pelletier for her informal review of the manuscript. This project was supported by the USDA National Institute of Food and Agriculture through the Maine Agricultural & Forest Experiment Station: Hatch Project Numbers ME022102 and ME022329 (Ishaq) and ME022303 (Li) which supported Johanna Holman; the USDA-NIFA-AFRI Foundational Program [Li and Chen; USDA/NIFA 2018-67017-27520/2018-67017-36797]; and the National Institute of Health [Li and Ishaq; NIH/NIDDK 1R15DK133826-01] which supported Marissa Kinney, Timothy Hunt, and Benjamin Hunt. Lola Holcomb was supported by US National Science Foundation One Health and the Environment (OG&E): Convergence of Social and Biological Sciences NRT program grant DGE-1922560, and through the UMaine Graduate School of Biomedical Sciences and Engineering.

Author Contributions

Conceptualization, S.L.I., Y.L., T.Z., G.C., G.M; Methodology, S.L.I., Y.L., T.Z., G.M., P.M., J.H.; Software, S.L.I.; Formal Analysis, J.H., M.K., S.L.I., T.H., B.H.; Investigation, J.H., L.C., J.B.; G.C., D.B.; Resources, S.L.I., Y.L., T.Z.; Data Curation, S.L.I., J.H.; Writing - Original Draft, J.H., L.C., S.L.I., Y.L.; Writing - Review and Editing; S.L.I., Y.L., T.Z., G.M., P.M., J.H., L.C., J.B., G.C., D.B., T.H., B.H., L.H. M.K.; Visualization, J.H., S.L.I., T.H., B.H.; Supervision, J.H., S.L.I., Y.L., T.Z.; Project Administration, S.L.I., Y.L., T.Z; Funding Acquisition, S.L.I., Y.L., T.Z., G.C.

809 **Figure Legends**

810 **Figure 1. Experimental design schematic for a chronic model of ulcerative colitis induced by**
811 **dextran sodium sulfate (DSS) in 40 male mice (C57BL/6) beginning at 7-weeks of age.**
812
813 **Figure 2. Body weights (A) and Disease Activity Index scores (B) in mice across a 34-day trial**
814 **under a DSS-induced model of chronic, relapsing colitis with or without 10% steamed**
815 **broccoli sprouts in diet.** Body weights and time scale were normalized to the day mice began the
816 broccoli sprout diet, set at 100% starting weight and Day 1, respectively. DAI scores are calculated
817 by weight loss intensity score, fecal blood, and fecal consistency. Treatment comparisons at each
818 day compared by ANOVA, and significance is designated as 0.001 '***'.
819
820 **Figure 3. Cytokines (A) and lipocalin (B) in plasma on the last day of the trial from mice**
821 **under a DSS-induced model of chronic, relapsing colitis with or without 10% steamed**
822 **broccoli sprouts in diet.** Cytokines include CCL4; interleukins IL-1β and IL-6; and tumor
823 necrosis factor alpha (TNF-α). Data are represented as mean ± SD. *, $p < 0.05$, ANOVA.

824 **Figure 4. Gut bacterial taxa identified from mice having a positive fecal occult blood score**
825 **at sacrifice under a DSS-induced model of chronic, relapsing colitis with or without 10%**
826 **steamed broccoli sprouts in diet.** Data were subset to mice with a positive score on the last day
827 of the experiment, when the gut samples were collected. Important features (SVs) were identified
828 through permutational random forest analysis, and only the features important to this group (>50
829 reads) are listed out of 143 significant ($p < 0.05$) features across all treatments. Model accuracy
830 was 89.7%. Bacterial sequence variants (SV) are identified as the lowest level of taxonomic
831 identity possible, with "NA" indicating which could not be identified to species, and the number
832 indicating which specific SV it was.

833 **Figure 5. Observed bacterial richness along the intestine of mice under a DSS-induced model**
834 **of chronic, relapsing colitis with or without 10% steamed broccoli sprouts in diet.** Richness
835 is calculated as the number of different bacterial sequence variants (SVs). Statistically significant
836 comparisons are provided in Table 1.
837
838 **Figure 6. Principal coordinate analysis of bacterial community similarity along the intestines**
839 **of mice under a DSS-induced model of chronic, relapsing colitis with or without 10%**
840 **steamed broccoli sprouts in diet.** Panel A was calculated with unweighted Jaccard Similarity to
841 visualize differences in the taxonomic structure, and panel B with weighted Bray-Curtis to
842 visualize structure and abundance.
843
844 **Figure 7. Principal coordinate analysis of bacterial communities from locations along the**
845 **intestines of mice under a DSS-induced model of chronic, relapsing colitis with or without**
846 **10% steamed broccoli sprouts in diet: (A) All treatments (B) Control+DSS only.** Bacterial
847 communities in the jejunum, cecum, and colon were statistically different (permANOVA, $p < 0.05$)
848 from each other in the treatment groups (A) Control, Broccoli, and Broccoli+DSS, were not
849 statistically different from each other after multiple bouts of colitis in the (B) Control+DSS group.
850

851 **Figure 8. Bacterial sequence variants (SVs) belonging to the genera which have putative**
852 **capacity to convert glucoraphanin to sulforaphane for mice under a DSS-induced model of**
853 **chronic, relapsing colitis with or without 10% steamed broccoli sprouts in diet.** Strains of
854 bacteria in these genera have been demonstrated to perform myrosinase-like activity in the
855 digestive tract, as reviewed in (43). Four treatment groups were used in a 34-day chronic,
856 relapsing model of colitis: control diet, control diet with DSS added to drinking water, control
857 diet adjusted with 10% by weight steamed broccoli sprouts, and 10% broccoli sprout diet with
858 DSS added to drinking water.
859
860 **Figure 9. Biogeography of the dominant *Bacteroides* SV (*B.*-dominant) in the gut (A) and**
861 **abundance of reads belonging to *Bacteroides* species by diet treatment and anatomical**
862 **location in the gastrointestinal tract of mice.** (A) *B.*-dominant was present in the jejunum
863 contents and scrapings and abundant in the cecum contents, colon contents, and colon scrapings.
864 DSS reduced *B.*-dominant colon content density. (B) The Silva Database identified *Bacteroides*
865 species *acidifaciens*, *massiliensis*, and *sartorii*. Of the BLASTN identified species for *B.*-dominant
866 SVs, only *B. thetaiotaomicron* was associated with broccoli-sprout-fed mice.
867
868 **Figure 10: Prevalence of the operon BT2159-BT2156 in *Bacteroides thetaiotaomicron* (VPI-**
869 **5482) in mice with and without chronic, relapsing DSS-induced colitis where diet was**
870 **manipulated.** Percentages are based on the number of samples (by diet and anatomical location)
871 in each category of gene abundance (minimum mean copy numbers: red low <100, purple medium
872 100-100,000, blue high >100,000) across all 5 genes in the operon.
873

874 **Table Legends**

875 **Table 1. Statistical comparison of observed richness along the intestine of mice under a DSS-**
876 **induced model of chronic, relapsing colitis with or without 10% steamed broccoli sprouts in**
877 **diet.** Comparisons were made using linear regression models comparing treatment, in subsets of
878 the data by anatomical location. Only significant comparisons ($p < 0.05$) are listed. Bacterial
879 richness is visualized in Figure 5.

880

881 **Supplemental Materials Legends**

882
883 **Supplemental Figures and Table.** Additional data visualizations are included to demonstrate
884 minor points or null results.
885
886 **Supplemental Material.** The R code that was used to clean, visualize, and statistically analyze
887 the bacterial community sequencing data presented.
888

889 **References**

890 1. Peery AF, Crockett SD, Murphy CC, Lund JL, Dellon ES, Williams JL, Jensen ET,
891 Shaheen NJ, Barritt AS, Lieber SR, Kochar B, Barnes EL, Fan YC, Pate V, Galanko J,
892 Baron TH, Sandler RS. 2019. Burden and Cost of Gastrointestinal, Liver, and Pancreatic
893 Diseases in the United States: Update 2018. Gastroenterology 156:254–272.e11.

894 2. Singh S, Qian AS, Nguyen NH, Ho SKM, Luo J, Jairath V, Sandborn WJ, Ma C. 2022.
895 Trends in U.S. Health Care Spending on Inflammatory Bowel Diseases, 1996-2016.
896 Inflamm Bowel Dis 28:364–372.

897 3. Lu Q, Yang M-F, Liang Y-J, Xu J, Xu H-M, Nie Y-Q, Wang L-S, Yao J, Li D-F. 2022.
898 Immunology of Inflammatory Bowel Disease: Molecular Mechanisms and Therapeutics. J
899 Inflamm Res 15:1825–1844.

900 4. Rubin DC, Shaker A, Levin MS. 2012. Chronic intestinal inflammation: Inflammatory
901 bowel disease and colitis-associated colon cancer. Frontiers in Immunology 3:00107.

902 5. Walker RE, Keane CR, Burke JG. 2010. Disparities and access to healthy food in the
903 United States: A review of food deserts literature. Health Place 16:876–884.

904 6. Banerjee S, Ghosh S, Sinha K, Chowdhury S, Sil PC. 2019. Sulphur dioxide ameliorates
905 colitis related pathophysiology and inflammation. Toxicology 412:63–78.

906 7. Lewis JD, Abreu MT. 2017. Diet as a Trigger or Therapy for Inflammatory Bowel Diseases.
907 Gastroenterology 152:398–414.e6.

908 8. Armstrong HK, Bording-Jorgensen M, Santer DM, Zhang Z, Valcheva R, Rieger AM,

909 Sung-Ho Kim J, Dijk SI, Mahmood R, Ogungbola O, Jovel J, Moreau F, Gorman H,
910 Dickner R, Jerasi J, Mander IK, Lafleur D, Cheng C, Petrova A, Jeanson T-L, Mason A,
911 Sergi CM, Levine A, Chadee K, Armstrong D, Rauscher S, Bernstein CN, Carroll MW,
912 Huynh HQ, Walter J, Madsen KL, Dieleman LA, Wine E. 2022. Unfermented β-fructan
913 Fibers Fuel Inflammation in Select Inflammatory Bowel Disease Patients. Gastroenterology
914 https://doi.org/10.1053/j.gastro.2022.09.034.

915 9. Tse G, Eslick GD. 2014. Cruciferous vegetables and risk of colorectal neoplasms: a
916 systematic review and meta-analysis. Nutr Cancer 66:128–139.

917 10. Li Y, Zhang T, Schwartz SJ, Sun D. 2011. Sulforaphane Potentiates the Efficacy of 17-
918 Allylamino 17-Demethoxygeldanamycin Against Pancreatic Cancer Through Enhanced
919 Abrogation of Hsp90 Chaperone Function. Nutrition and Cancer
920 https://doi.org/10.1080/01635581.2011.596645.

921 11. Li Y, Zhang T, Korkaya H, Liu S, Lee H-F, Newman B, Yu Y, Clouthier SG, Schwartz SJ,
922 Wicha MS, Sun D. 2010. Sulforaphane, a dietary component of broccoli/broccoli sprouts,
923 inhibits breast cancer stem cells. Clin Cancer Res 16:2580–2590.

924 12. Angelino D, Jeffery E. 2014. Glucosinolate hydrolysis and bioavailability of resulting
925 isothiocyanates: Focus on glucoraphanin. J Funct Foods 7:67–76.

926 13. Zhang T, Holman J, McKinstry D, Trindade BC, Eaton KA, Mendoza-Castrejon J, Ho S,
927 Wells E, Yuan H, Wen B, Sun D, Chen GY, Li Y. 2022. A steamed broccoli sprout diet
928 preparation that reduces colitis via the gut microbiota. J Nutr Biochem 112:109215.

929 14. Fahey JW, Stephenson KK, Wade KL, Talalay P. 2013. Urease from *Helicobacter pylori* is

930 inactivated by sulforaphane and other isothiocyanates. Biochem Biophys Res Commun
931 435:1–7.

932 15. Fahey JW, Wehage SL, Holtzclaw WD, Kensler TW, Egner PA, Shapiro TA, Talalay P.
933 2012. Protection of humans by plant glucosinolates: efficiency of conversion of
934 glucosinolates to isothiocyanates by the gastrointestinal microflora. Cancer Prev Res (Phila)
935 5:603–611.

936 16. Wei L-Y, Zhang J-K, Zheng L, Chen Y. 2022. The functional role of sulforaphane in
937 intestinal inflammation: a review. Food Funct 13:514–529.

938 17. Holman J, Hurd M, Moses P, Mawe G, Zhang T, Ishaq SL, Li Y. 2023. Interplay of
939 Broccoli/Broccoli Sprout Bioactives with Gut Microbiota in Reducing Inflammation in
940 Inflammatory Bowel Diseases. J Nutr Biochem 113:109238.

941 18. Zhang Y, Tan L, Li C, Wu H, Ran D, Zhang Z. 2020. Sulforaphane alter the microbiota and
942 mitigate colitis severity on mice ulcerative colitis induced by DSS. AMB Express 10:119.

943 19. Li Y, Wicha MS, Schwartz SJ, Sun D. 2011. Implications of cancer stem cell theory for
944 cancer chemoprevention by natural dietary compounds. J Nutr Biochem 22:799–806.

945 20. Bricker GV, Riedl KM, Ralston RA, Tober KL, Oberyszyn TM, Schwartz SJ. 2014.
946 Isothiocyanate metabolism, distribution, and interconversion in mice following
947 consumption of thermally processed broccoli sprouts or purified sulforaphane. Mol Nutr
948 Food Res 58:1991–2000.

949 21. Liou CS, Sirk SJ, Diaz CAC, Klein AP, Fischer CR, Higginbottom SK, Erez A, Donia MS,

950 Sonnenburg JL, Sattely ES. 2020. A Metabolic Pathway for Activation of Dietary
951 Glucosinolates by a Human Gut Symbiont. Cell 180:717–728.e19.

952 22. Elfoul L, Rabot S, Khelifa N, Quinsac A, Duguay A, Rimbault A. 2001. Formation of allyl
953 isothiocyanate from sinigrin in the digestive tract of rats monoassociated with a human
954 colonic strain of *Bacteroides thetaiotaomicron*. FEMS Microbiol Lett 197:99–103.

955 23. Shapiro TA, Fahey JW, Wade KL, Stephenson KK, Talalay P. 1998. Human metabolism
956 and excretion of cancer chemoprotective glucosinolates and isothiocyanates of cruciferous
957 vegetables. Cancer Epidemiol Biomarkers Prev 7:1091–1100.

958 24. Yagishita Y, Fahey JW, Dinkova-Kostova AT, Kensler TW. 2019. Broccoli or
959 Sulforaphane: Is It the Source or Dose That Matters? Molecules 24:3593.

960 25. Li F, Hullar MAJ, Beresford SAA, Lampe JW. 2011. Variation of glucoraphanin
961 metabolism in vivo and ex vivo by human gut bacteria. Br J Nutr 106:408–416.

962 26. Lai R-H, Miller MJ, Jeffery E. 2010. Glucoraphanin hydrolysis by microbiota in the rat
963 cecum results in sulforaphane absorption. Food Funct 1:161–166.

964 27. Johnson AJ, Vangay P, Al-Ghalith GA, Hillmann BM, Ward TL, Shields-Cutler RR, Kim
965 AD, Shmagel AK, Syed AN, Personalized Microbiome Class Students, Walter J, Menon R,
966 Koecher K, Knights D. 2019. Daily Sampling Reveals Personalized Diet-Microbiome
967 Associations in Humans. Cell Host Microbe 25:789–802.e5.

968 28. Amato KR, Arrieta M-C, Azad MB, Bailey MT, Broussard JL, Bruggeling CE, Claud EC,
969 Costello EK, Davenport ER, Dutilh BE, Swain Ewald HA, Ewald P, Hanlon EC, Julion W,

970 Keshavarzian A, Maurice CF, Miller GE, Preidis GA, Segurel L, Singer B, Subramanian S,
971 Zhao L, Kuzawa CW. 2021. The human gut microbiome and health inequities. Proc Natl
972 Acad Sci U S A 118:e2017947118.

973 29. Hillman ET, Lu H, Yao T, Nakatsu CH. 2017. Microbial Ecology along the Gastrointestinal
974 Tract. Microbes Environ 32:300–313.

975 30. Lynch SV, Pedersen O. 2016. The Human Intestinal Microbiome in Health and Disease. N
976 Engl J Med 375:2369–2379.

977 31. Pereira FC, Berry D. 2017. Microbial nutrient niches in the gut. Environ Microbiol
978 19:1366–1378.

979 32. Press AG, Hauptmann IA, Hauptmann L, Fuchs B, Fuchs M, Ewe K, Ramadori G. 1998.
980 Gastrointestinal pH profiles in patients with inflammatory bowel disease. Aliment
981 Pharmacol Ther 12:673–678.

982 33. Compare D, Pica L, Rocco A, De Giorgi F, Cuomo R, Sarnelli G, Romano M, Nardone G.
983 2011. Effects of long-term PPI treatment on producing bowel symptoms and SIBO.
984 European Journal of Clinical Investigation https://doi.org/10.1111/j.1365-
985 2362.2010.02419.x.

986 34. Swidsinski A, Ladhoff A, Pernthaler A, Swidsinski S, Loening-Baucke V, Ortner M, Weber
987 J, Hoffmann U, Schreiber S, Dietel M, Lochs H. 2002. Mucosal flora in inflammatory
988 bowel disease. Gastroenterology 122:44–54.

989 35. Gevers D, Kugathasan S, Denson LA, Vázquez-Baeza Y, Van Treuren W, Ren B, Schwager

990 E, Knights D, Song SJ, Yassour M, Morgan XC, Kostic AD, Luo C, González A,
991 McDonald D, Haberman Y, Walters T, Baker S, Rosh J, Stephens M, Heyman M,
992 Markowitz J, Baldassano R, Griffiths A, Sylvester F, Mack D, Kim S, Crandall W, Hyams
993 J, Huttenhower C, Knight R, Xavier RJ. 2014. The treatment-naive microbiome in new-
994 onset Crohn's disease. Cell Host Microbe 15:382–392.

995 36. Kozik AJ, Nakatsu CH, Chun H, Jones-Hall YL. 2019. Comparison of the fecal, cecal, and
996 mucus microbiome in male and female mice after TNBS-induced colitis. PLoS One
997 14:e0225079.

998 37. Xu P, Lv T, Dong S, Cui Z, Luo X, Jia B, Jeon CO, Zhang J. 2022. Association between
999 intestinal microbiome and inflammatory bowel disease: Insights from bibliometric analysis.
1000 Comput Struct Biotechnol J 20:1716–1725.

1001 38. Boger-May A, Reed T, LaTorre D, Ruley-Haase K, Hoffman H, English L, Roncagli C,
1002 Overstreet A-M, Boone D. 2022. Altered microbial biogeography in an innate model of
1003 colitis. Gut Microbes 14:2123677.

1004 39. da Costa Goncalves F, Schneider N, Mello HF, Passos EP, da Rosa Paz AH. 2013.
1005 Characterization of Acute Murine Dextran Sodium Sulfate (DSS) Colitis: Severity of
1006 Inflammation is Dependent on the DSS Molecular Weight and Concentration. Acta
1007 Scientiae Veterinari 41:1–9.

1008 40. Wirtz S, Popp V, Kindermann M, Gerlach K, Weigmann B, Fichtner-Feigl S, Neurath MF.
1009 2017. Chemically induced mouse models of acute and chronic intestinal inflammation. Nat
1010 Protoc 12:1295–1309.

1011 41. Eichele DD, Kharbanda KK. 2017. Dextran sodium sulfate colitis murine model: An
1012 indispensable tool for advancing our understanding of inflammatory bowel diseases
1013 pathogenesis. World J Gastroenterol 23:6016–6029.

1014 42. Gong W, Yu J, Zheng T, Liu P, Zhao F, Liu J, Hong Z, Ren H, Gu G, Wang G, Wu X, Zhao
1015 Y, Ren J. 2021. CCL4-mediated targeting of spleen tyrosine kinase (Syk) inhibitor using
1016 nanoparticles alleviates inflammatory bowel disease. Clin Transl Med 11:e339.

1017 43. Sikorska-Zimny K, Beneduce L. 2021. The Metabolism of Glucosinolates by Gut
1018 Microbiota. Nutrients 13:2750.

1019 44. Luang-In V, Narbad A, Cebeci F, Bennett M, Rossiter JT. 2015. Identification of Proteins
1020 Possibly Involved in Glucosinolate Metabolism in *L. agilis* R16 and *E. coli* VL8. Protein J
1021 34:135–146.

1022 45. Chénard T, Malick M, Dubé J, Massé E. 2020. The influence of blood on the human gut
1023 microbiome. BMC Microbiol 20:44.

1024 46. Cafiero C, Re A, Pisconti S, Trombetti M, Perri M, Colosimo M, D'Amato G, Gallelli L,
1025 Cannataro R, Molinario C, Fazio A, Caroleo MC, Cione E. 2020. Dysbiosis in intestinal
1026 microbiome linked to fecal blood determined by direct hybridization. 3 Biotech 10:358.

1027 47. Chassaing B, Srinivasan G, Delgado MA, Young AN, Gewirtz AT, Vijay-Kumar M. 2012.
1028 Fecal Lipocalin 2, a Sensitive and Broadly Dynamic Non-Invasive Biomarker for Intestinal
1029 Inflammation. PLoS One 7:e44328.

1030 48. Bábíčková J, Tóthová Ľ, Lengyelová E, Bartoňová A, Hodosy J, Gardlík R, Celec P. 2015.

1031 Sex Differences in Experimentally Induced Colitis in Mice: a Role for Estrogens.
1032 Inflammation 38:1996–2006.

1033 49. Goodman WA, Havran HL, Quereshy HA, Kuang S, De Salvo C, Pizarro TT. 2018.
1034 Estrogen Receptor α Loss-of-Function Protects Female Mice From DSS-Induced
1035 Experimental Colitis. Cell Mol Gastroenterol Hepatol 5:630–633.e1.

1036 50. Letourneau J, Holmes ZC, Dallow EP, Durand HK, Jiang S, Carrion VM, Gupta SK,
1037 Mincey AC, Muehlbauer MJ, Bain JR, David LA. 2022. Ecological memory of prior
1038 nutrient exposure in the human gut microbiome. ISME J 16:2479–2490.

1039 51. Angelino D, Dosz EB, Sun J, Hoeflinger JL, Van Tassell ML, Chen P, Harnly JM, Miller
1040 MJ, Jeffery EH. 2015. Myrosinase-dependent and -independent formation and control of
1041 isothiocyanate products of glucosinolate hydrolysis. Front Plant Sci 6:831.

1042 52. Stackebrandt E, Kramer I, Swiderski J, Hippe H. 1999. Phylogenetic basis for a taxonomic
1043 dissection of the genus *Clostridium*. FEMS Immunol Med Microbiol 24:253–258.

1044 53. Uzal FA, McClane BA, Cheung JK, Theoret J, Garcia JP, Moore RJ, Rood JI. 2015. Animal
1045 models to study the pathogenesis of human and animal *Clostridium perfringens* infections.
1046 Vet Microbiol 179:23–33.

1047 54. Chen H, Ma X, Liu Y, Ma L, Chen Z, Lin X, Si L, Ma X, Chen X. 2019. Gut Microbiota
1048 Interventions With *Clostridium butyricum* and Norfloxacin Modulate Immune Response in
1049 Experimental Autoimmune Encephalomyelitis Mice. Front Immunol 10:1662.

1050 55. Shahinozzaman M, Raychaudhuri S, Fan S, Obanda DN. 2021. Kale Attenuates

1051 Inflammation and Modulates Gut Microbial Composition and Function in C57BL/6J Mice
1052 with Diet-Induced Obesity. Microorganisms 9:238.

1053 56. Ju T, Kong JY, Stothard P, Willing BP. 2019. Defining the role of *Parasutterella*, a
1054 previously uncharacterized member of the core gut microbiota. ISME J 13:1520–1534.

1055 57. Hubbard TD, Murray IA, Nichols RG, Cassel K, Podolsky M, Kuzu G, Tian Y, Smith P,
1056 Kennett MJ, Patterson AD, Perdew GH. 2017. Dietary Broccoli Impacts Microbial
1057 Community Structure and Attenuates Chemically Induced Colitis in Mice in an Ah receptor
1058 dependent manner. J Funct Foods 37:685–698.

1059 58. Antonson AM, Evans MV, Galley JD, Chen HJ, Rajasekera TA, Lammers SM, Hale VL,
1060 Bailey MT, Gur TL. 2020. Unique maternal immune and functional microbial profiles
1061 during prenatal stress. Sci Rep 10:20288.

1062 59. Huarte-Mendicoa JC, Astiasarán I, Bello J. 1997. Nitrate and nitrite levels in fresh and
1063 frozen broccoli. Effect of freezing and cooking. Food Chem 58:39–42.

1064 60. Araki Y, Mukaisho K, Sugihara H, Fujiyama Y, Hattori T. 2010. *Proteus mirabilis* sp.
1065 intestinal microflora grow in a dextran sulfate sodium-rich environment. Int J Mol Med
1066 25:203–208.

1067 61. Chang C-S, Liao Y-C, Huang C-T, Lin C-M, Cheung CHY, Ruan J-W, Yu W-H, Tsai Y-T,
1068 Lin I-J, Huang C-H, Liou J-S, Chou Y-H, Chien H-J, Chuang H-L, Juan H-F, Huang H-C,
1069 Chan H-L, Liao Y-C, Tang S-C, Su Y-W, Tan T-H, Bäumler AJ, Kao C-Y. 2021.
1070 Identification of a gut microbiota member that ameliorates DSS-induced colitis in intestinal
1071 barrier enhanced Dusp6-deficient mice. Cell Rep 37:110016.

1072 62. Khan I, Bai Y, Ullah N, Liu G, Rajoka MSR, Zhang C. 2022. Differential Susceptibility of
1073 the Gut Microbiota to DSS Treatment Interferes in the Conserved Microbiome Association
1074 in Mouse Models of Colitis and Is Related to the Initial Gut Microbiota Difference.
1075 Advanced Gut & Microbiome Research 2022:7813278.

1076 63. Gibbons SM. 2020. Keystone taxa indispensable for microbiome recovery. Nature
1077 Microbiology 5:1067–1068.

1078 64. Duvallet C, Gibbons SM, Gurry T, Irizarry RA, Alm EJ. 2017. Meta-analysis of gut
1079 microbiome studies identifies disease-specific and shared responses. Nat Commun 8:1784.

1080 65. Walters WA, Xu Z, Knight R. 2014. Meta-analyses of human gut microbes associated with
1081 obesity and IBD. FEBS Lett 588:4223–4233.

1082 66. Han YW. 2015. *Fusobacterium nucleatum*: a commensal-turned pathogen. Curr Opin
1083 Microbiol 23:141–147.

1084 67. Tropini C, Earle KA, Huang KC, Sonnenburg JL. 2017. The Gut Microbiome: Connecting
1085 Spatial Organization to Function. Cell Host Microbe 21:433–442.

1086 68. Gu M, Samuelson DR, de la Rua NM, Charles TP, Taylor CM, Luo M, Siggins RW,
1087 Shellito JE, Welsh DA. 2022. Host innate and adaptive immunity shapes the gut microbiota
1088 biogeography. Microbiol Immunol 66:330–341.

1089 69. Suzuki TA, Nachman MW. 2016. Spatial Heterogeneity of Gut Microbial Composition
1090 along the Gastrointestinal Tract in Natural Populations of House Mice. PLoS One
1091 11:e0163720.

1092 70. Wu S, Zhang B, Liu Y, Suo X, Li H. 2018. Influence of surface topography on bacterial
1093 adhesion: A review (Review). Biointerphases 13:060801.

1094 71. Stenman LK, Holma R, Forsgård R, Gylling H, Korpela R. 2013. Higher fecal bile acid
1095 hydrophobicity is associated with exacerbation of dextran sodium sulfate colitis in mice. J
1096 Nutr 143:1691–1697.

1097 72. Fahey JW, Smilovitz Burak J, Evans D. 2022. Sprout microbial safety: A reappraisal after a
1098 quarter-century. Food Frontiers 1–7.

1099 73. Rao M, Afshin A, Singh G, Mozaffarian D. 2013. Do healthier foods and diet patterns cost
1100 more than less healthy options? A systematic review and meta-analysis. BMJ Open
1101 3:e004277.

1102 74. Economic Research Service. Food Access Research Atlas. US Department of Agriculture.
1103 https://www.ers.usda.gov/data/fooddesert. Retrieved 22 April 2022.

1104 75. Wedick NM, Ma Y, Olendzki BC, Procter-Gray E, Cheng J, Kane KJ, Ockene IS, Pagoto
1105 SL, Land TG, Li W. 2015. Access to healthy food stores modifies effect of a dietary
1106 intervention. Am J Prev Med 48:309–317.

1107 76. Baker EA, Schootman M, Barnidge E, Kelly C. 2006. The role of race and poverty in access
1108 to foods that enable individuals to adhere to dietary guidelines. Prev Chronic Dis 3:A76.

1109 77. Inotiv. TD.97184: AIN93G Diet. Inotiv. https://insights.envigo.com/hubfs/resources/data-
1110 sheets/97184.pdf. Retrieved 28 April 2023.

1111 78. Mähler M, Bristol IJ, Leiter EH, Workman AE, Birkenmeier EH, Elson CO, Sundberg JP.

1998. Differential susceptibility of inbred mouse strains to dextran sulfate sodium-induced colitis. Am J Physiol 274:G544–51.

79. Okayasu I, Hatakeyama S, Yamada M, Ohkusa T, Inagaki Y, Nakaya R. 1990. A novel method in the induction of reliable experimental acute and chronic ulcerative colitis in mice. Gastroenterology 98:694–702.

80. Poritz LS, Garver KI, Green C, Fitzpatrick L, Ruggiero F, Koltun WA. 2007. Loss of the tight junction protein ZO-1 in dextran sulfate sodium induced colitis. J Surg Res 140:12–19.

81. Chassaing B, Aitken JD, Malleshappa M, Vijay-Kumar M. 2014. Dextran sulfate sodium (DSS)-induced colitis in mice. Curr Protoc Immunol 104:15.25.1–15.25.14.

82. Araki A, Kanai T, Ishikura T, Makita S, Uraushihara K, Iiyama R, Totsuka T, Takeda K, Akira S, Watanabe M. 2005. MyD88-deficient mice develop severe intestinal inflammation in dextran sodium sulfate colitis. J Gastroenterol 40:16–23.

83. Dieleman LA, Ridwan BU, Tennyson GS, Beagley KW, Bucy RP, Elson CO. 1994. Dextran sulfate sodium-induced colitis occurs in severe combined immunodeficient mice. Gastroenterology 107:1643–1652.

84. Taghipour N, Molaei M, Mosaffa N, Rostami-Nejad M, Asadzadeh Aghdaei H, Anissian A, Azimzadeh P, Zali MR. 2016. An experimental model of colitis induced by dextran sulfate sodium from acute progresses to chronicity in C57BL/6: correlation between conditions of mice and the environment. Gastroenterol Hepatol Bed Bench 9:45–52.

85. Yu W, Li Q, Shao C, Zhang Y, Kang C, Zheng Y, Liu X, Liu X, Yan J. 2022. The Cao-

1132 Xiang-Wei-Kang formula attenuates the progression of experimental colitis by restoring the
1133 homeostasis of the microbiome and suppressing inflammation. Front Pharmacol 13:946065.

1134 86. Prakash T, Janadri S. 2022. Anti-inflammatory effect of wedelolactone on DSS induced
1135 colitis in rats: IL-6/STAT3 signaling pathway. J Ayurveda Integr Med 100544.

1136 87. Gobert AP, Al-Greene NT, Singh K, Coburn LA, Sierra JC, Verriere TG, Luis PB,
1137 Schneider C, Asim M, Allaman MM, Barry DP, Cleveland JL, Destefano Shields CE,
1138 Casero RA Jr, Washington MK, Piazuelo MB, Wilson KT. 2018. Distinct
1139 Immunomodulatory Effects of Spermine Oxidase in Colitis Induced by Epithelial Injury or
1140 Infection. Front Immunol 9:1242.

1141 88. Nocker A, Sossa-Fernandez P, Burr MD, Camper AK. 2007. Use of propidium monoazide
1142 for live/dead distinction in microbial ecology. Appl Environ Microbiol 73:5111–5117.

1143 89. The Earth Microbiome Project. 2022. The Earth Microbiome Project. The Earth
1144 Microbiome Project. https://earthmicrobiome.org/. Retrieved 22 April 2022.

1145 90. Callahan BJ, McMurdie PJ, Rosen MJ, Han AW, Johnson AJA, Holmes SP. 2016. DADA2:
1146 High-resolution sample inference from Illumina amplicon data. Nat Methods 13:581–583.

1147 91. RCoreTeam. 2022. R: a language and environment for statistical computing (4.2.2). R
1148 Foundation for Statistical Computing, Vienna, Austria. https://www.r-project.org/.

1149 92. Pruesse E, Quast C, Knittel K, Fuchs BM, Ludwig W, Peplies J, Glöckner FO. 2007.
1150 SILVA: a comprehensive online resource for quality checked and aligned ribosomal RNA
1151 sequence data compatible with ARB. Nucleic Acids Res 35:7188–7196.

93. Wickham H, Francois R, Henry L, Müller K. 2015. dplyr: A Grammar of Data Manipulation. R package version 0.4. 3. R Found Stat Comput , Vienna https://CRAN R-project org/package= dplyr.

94. Ishaq SL. 2017. Phyloseq_dealing_with_neg_controls_ Ishaq_example.R. Github. https://github.com/SueIshaq/Examples-DADA2-Phyloseq. Retrieved 5 March 2019.

95. McMurdie PJ, Holmes S. 2013. phyloseq: An R Package for Reproducible Interactive Analysis and Graphics of Microbiome Census Data. PLoS One 8:e61217.

96. Bates D, Mächler M, Zurich E, Bolker BM, Walker SC. 2015. Fitting Linear Mixed-Effects Models Using lme4. Journal of Statistical Software, Articles 67:1–48.

97. Pedersen EJ, Miller DL, Simpson GL, Ross N. 2019. Hierarchical generalized additive models: an introduction with mgcv. PeerJ 7:e6876.

98. Oksanen J, Guillaume Blanchet F, Friendly M, Kindt R, Legendre P, McGlinn D, Minchin PR, O'Hara RB, Simpson GL, Solymos P, Stevens MHH, Szoecs E, Wagner H. 2020. Vegan: Community Ecology Package (2.5-7). https://cran.r-project.org/web/packages/vegan/vignettes/diversity-vegan.pdf.

99. Archer E. 2022. rfpermute: Estimate Permutation p-Values for Random Forest Importance Metrics (2.5.1). https://github.com/EricArcher/rfPermute.

100. Wickham H. 2016. ggplot2: Elegant graphics for Data Analysis. Springer Publishing Company, New York. https://dl.acm.org/citation.cfm?id=1795559.

101. Kassambara A. 2022. ggpubr:"ggplot2" based publication ready plots (0.1.7).

1172 https://rpkgs.datanovia.com/ggpubr/.

1173 102. Knights D, Kuczynski J, Charlson ES, Zaneveld J, Mozer MC, Collman RG, Bushman
1174 FD, Knight R, Kelley ST. 2011. Bayesian community-wide culture-independent microbial
1175 source tracking. Nat Methods 8:761–763.

1176 103. Galey M. 2021. Mi-Seq Analysis. GitHub. https://mgaley-004.github.io/MiSeq-
1177 Analysis/Tutorials/SourceSink.html, https://github.com/mgaley-004/MiSeq-Analysis.
1178 Retrieved 7 December 2022.

1179